Oceanological and Hydrobiological Studies

International Journal of Oceanography and Hydrobiology

Volume 52, No. 1 March 2023
pages (20-40)

sciendo

ISSN 1730-413X
eISSN 1897-3191

Effects of the tide on the temporal and spatial physicochemical structure of the Kienké river estuary (South Atlantic Coast of Cameroon, Kribi) and its phytoplankton

by

Anselme Crépin MAMA*[,1,2], Gisele Flodore Youbouni GHEPDEU[3], Olivia FOSSI TANKOUA[1,2], Manfred Desire BONGA[1,2], Willy Karol ABOUGA BODO[1,2], Thérésa Irma MANDENG[1,2], François Désiré OWONA EDOA[2,4], Noel Chuye TANGKO[2], Jules Rémi NGOUPAYOU NDAM[5]

DOI: **https://doi.org/10.26881/oahs-2023.1.02**
Category: **Original research paper**
Received: **September 11, 2022**
Accepted: **November 29, 2022**

[1]*Department of Oceanography, Institute of Fischeries and Aquatic Sciences, The University of Douala, Cameroon*

[2]*Association of Professionals in Coastal and Aquatics Management, Po Box 274, Yaoundé*

[3]*Specialized Center for Research on Marine Ecosystems, IRAD Kribi, Cameroon*

[4]*Laboratry of Hydrobiology and Environment in Faculty of Sciences, University of Yaoundé 1*

[5]*Department of Earth Sciences, Faculty of Science, University of Yaounde 1, Cameroon*

* Corresponding author: mamacrepin@yahoo.fr

Abstract

The present work aimed to understand the physicochemical and phytoplanktonic structure of the Kienke estuary water in the urban area of Kribi town in relation to human activities and fluvial or oceanic influences. Field investigations and laboratory work were devoted to the sampling and measurement of some physicochemical and biological parameters, specific treatments and classical statistics (descriptive, multidimensional) of variables. Estuary water is characterised by an instability and spatio-temporal variations in its physicochemical parameters. The most sensitive parameters are as follows: a temperature ranging between 22.6°C and 31°C under the influence of atmospheric variations, electrical conductivity and salinity that are relatively high ($0.22 < C. E < 49.70$ mS cm^{-1}; avg =16.56 mS cm^{-1}; $0 < Sal < 29.32$ PSU; avg = 11.51 PSU), and a pH that is overall acidic to basic ($6 < pH < 8.86$; avg = 7.75 ± 0.82). The nutrients variation (ammonium, nitrite, nitrate and orthophosphate) is very low in space and time, with a longitudinal distribution controlled by tidal flows, river flows and the biological pump. For the 64 samples collected, 167 phytoplankton taxa were identified. The most abundant (36.36%) were Chrysophyta Division, followed by Chlorophyta. Species richness is marked by brackish water taxa. According to this structure and the combination of both gradients, mineratilisation and organic matter enrichment is of a physicochemical typology, and the biotypology is hydrotypologically dependent.

Key words: Kienké estuary, phytoplankton, physicochemistry, typologies, fluvial and oceanic dynamics, human activities

1. Introduction

Coastal zones are complex and fragile ecosystems where the interaction between the marine and terrestrial parts is manifest. Economic and social issues have made them privileged areas for human activities such as shipping, urbanisation, industrialisation, tourism, fishing and maritime transport (Ducotroy et al. 2016; Cereja et al. 2022). The overall environmental problems of these areas are linked to the convergence of several types of pollution (physical, chemical, biological). In addition to anthropogenic and natural pressures, coastal areas are also vulnerable to climate change. (McLusky & Elliott 2004; Suman et al. 2012; Ong & Ransangan 2018; Cereja et al. 2021).

Cameroon, like other countries with an oceanic coastline, is concerned about all of the above. Its coastal zone is a geostrategic area judged from an environmental, social and economic perspective (MINEF-CMEF 2005; ENVI-REP Cmr 2011). Thus, in its structuring plan, the State of Cameroon has located numerous development and industrial projects on the southern part of its Atlantic coast (the deepwater port of Kribi, the Kribi gas power plant, several cement factories, agro-industries, fisheries) (Folack et al. 2011). Through all these existing infrastructures or those under construction, Kribi has become an El Dorado for job seekers, tourists, traders and many others. Statistical models indicate that the population of the three Cameroon Coastal Regions is expected to reach 6,751,890 in 2025 and 9,367,680 by 2050 (BUCREP 2010).

This rapid growth creates significant pressure on these coastal and marine environments, marked by water and soil pollution and mangrove destruction (Ekane & Oben 2001; Djama 1992; Casé et al. 2008; Folack 2010). The socio-economic value of Cameroon's coastal ecosystems explains the fact that their scientific study began quite early, with several specific works (Monod 1928; Crosnier 1964). Some studies on the assessment of estuarine biodiversity (Folack et al. 2009, Fretey et al. 2022) and the dynamics of fisheries in the Cameroonian estuarine systems (Kebe et al. 1993; Djama 1994; Njifonjou 1998) has been carried out. However, very few studies specific to water quality in these environments have been carried out despite all the services provided. Existing information concerns the quantitative approach to biodegradation in the freshwater-saltwater mixing zone in the Sanaga and Nyong estuaries, and in the rivers of the Douala Bay (Giresse & Cahet 1997; Fonge et al. 2013; Mama et al. 2018; Mama et al. 2021).

However, water quality has an important influence on aquatic life, biodiversity and, more specifically, on phytoplankton, whose own changes can affect, among other things, its biomass, specific diversity and the biogeographical distribution of all species in the environment (Hernández-Fariñas & Bacher 2015). Hence the emergency to monitor the water resource for sustainable management (Singh et al. 2004; Yang et al. 2009; Oketola et al. 2013; Mama et al. 2018). However, the monitoring of aquatic environments has long been exclusively oriented towards the measurement of the physicochemical parameters of water. The limitations of these analyses in assessing the state of health of hydrosystems are recognised and stem from the fact that these analyses characterise the environment at the time of sampling and only provide very limited information on the impact of pollutants on the health and functioning of the ecosystem as a whole (Ruperd 1983; Blandin 1986).

A classical investigation of water quality therefore requires the combination of physicochemical variables and biological indicators (Jones et al. 2001; Casé et al. 2008; Gharib et al. 2011; Mama et al. 2018), in this case phytoplankton. Such a combination generally provides information on the health of estuarine waters and the conditions of evolution (Samocha & Lawrence 1995; Soininen 2002; Casé et al. 2008; Beyene et al. 2009). The choice of this biological indicator is related to its essential role in the functioning of the "biological pump" by fixing atmospheric CO_2 and thus contributing to regulating the Earth's climate (Tréguer et al. 2018; Owona et al. 2022), and also to phytoplankton primary production, which is a dimensional factor in the natural production of fish, molluscs and crustaceans, from which the world's fisheries extract 110 million tonnes each year (Zeller et al. 2018).

The Kienké River is very little documented. To date, in addition to work on the monograph of its watershed, it has been the subject of a few hydrological and geochemical studies in its upstream section (Olivry 1986; Liénou 2007). In the urban area of Kribi, the data on hydrobiology are fragmentary and refer only to either aquatic insects or freshwater shrimp (Tchakonté et al. 2014a; Tchakonté et al. 2014b; Makombu et al. 2015; Makombu et al. 2019). The present study was initiated to understand the physicochemical and phytoplanktonic structure of the Kienké estuary in relation to the anthropogenic activities present and the fluvial and oceanic influences (high and low tides). It aims firstly to determine the physicochemical and phytoplanktonic characteristics of the waters, and secondly to establish the physicochemical and phytoplanktonic typologies of the waters of the Kienké estuary.

2. Materials and methods

2.1. Presentation of study area

The Kienké estuary is part of the Campo-Nyong estuarine system of the Southern Atlantic Coast of Cameroon. It crosses the urban area of the port city of Kribi and is located between latitudes 02° 934' N and 02° 943' N and longitudes 09° 901' E and 09° 909' E (Figure 1). This area is subject to a Guinean equatorial climate, characterised by four seasons (Olivry 1986; Dzana 2011; Mama et al. 2018). The vegetation is diversified, with two major units: the Biafran forest, which is secondary and old evergreen, and the coastal forest composed of some degraded facies (fallows, scrubby recrusions) and vegetation facies influenced by the sea, such as monospecific plant formations with *Podococcus barteri* (Letouzey 1985; Nlend 2014). The geological formations of the area belong to two major lithological and structural units, namely the Archean core or basement of the Ntem, which is made up of plutono-metamorphic rocks, and the sedimentary formations. These weather to give soils of varying thicknesses and essentially yellow and red ferralitic soils crossed in places by hydromorphic soils (Lasserre et al. 1979; Maurizot et al. 1986; Nlend 2014; Aye et al. 2017; Ndjigui et al. 2018; Soh Tamehe et al. 2018).

2.2. Methods

In this study, some criteria were taken into account when choosing the sampling points on the site; among others:

- turbulence, when two water masses meet and there is the influence of the breakwater at the entrance to the channel of the small port of Kribi;
- the probable influence of point and diffuse sources of pollution from installations on the banks;
- the representativeness of the points with regard to environmental aspects likely to modify the structure of the hydrosystem;
- the expansion of the water plume into the sea after the mouth itself.

These criteria made it possible to define four (04) sampling points that were used to measure certain physicochemical parameters *in-situ*, to take water samples for laboratory analysis, and to sample phytoplankton during this study (Figure 1).

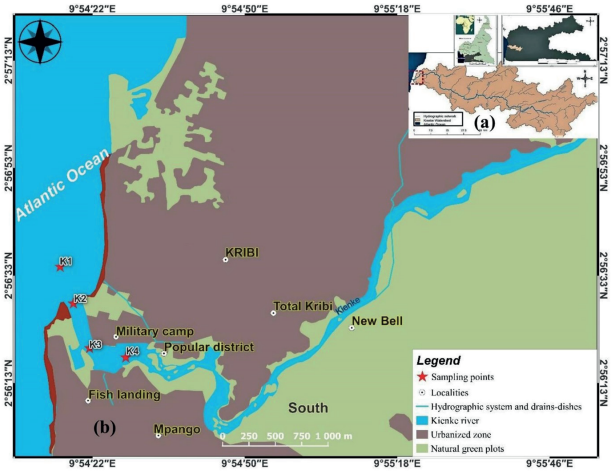

Figure 1

Study area in the Kienké river basin (a) and the sampling points in the estuary (b)

2.3. Sampling campaigns and laboratory analysis

Water samples used for physicochemical and biological analyses were collected between 2017 and 2018. All the seasons were covered during sampling as presented by Mama et al. (2018). For each season two samplings were carried out at each station during low tide and high tide respectively. Surface water was collected directly in a 1 l bottle. Deep water was collected using a 1.5 l Niskin bottle. Water samples destined for physicochemical analysis were stored in 1 liter double-capped polyethylene bottles and transported to the laboratory in an adiabatic enclosure at 4°C.

Physicochemical parameters were determined by the Aminot & Chaussepied (1983) method coupled with the standard methods of APHA (2005). Temperature, pH, conductivity, salinity and dissolved oxygen were recorded *in-situ*. Soluble reactive inorganic phosphorous (PO_4^{3-}), nitrites (NO_2^-), nitrates(NO_3^-), ammonium (NH_4^+), Total Suspended Solid (TSS), turbidity and Total Disolved solid (TDS) were measured/analysed in the laboratory using the spectrophotometer HACH DR/2800, following the standard methods described by Strickland & Parsons (1972), APHA (2005) and Rodier et al. (2009). A total of 64 water samples were collected for the phytoplankton analysis, 32 samples per tides. Surface water (50cm) was collected using a 1.5 L bottle. These samples were immediately fixed by lugol's iodine solution (5 ml), and left to stand for 24 hours, to allow decantation (Sournia 1978). Then the concentrate lower layer (25 ml) containing the sedimented algae was used for algae identification and counting in a

Malassez cell, using an Olympus optical microscope at 60× magnification. Identification of the phytoplankton species followed relevant text books and publications, including Iltis (1980), Botes (2001), Gopinathan et al. (2001), De Ba et al. (2006), Carmelo (1997), Verlencar & Desai (2004) and Karlson (2010).

2.4. Data analysis

2.4.1. Specific richness

The specific richness (S) is defined as the total number of identified species in a sample. This parameter can be a distinctive criterion of ecosystems or stations studied within a given ecosystem.

2.4.2. Statistical analysis

The influence of the tide on the various physicochemical parameters studied was tested for each station using the t-Student statistical test. To test the effect of the space represented by the stations, the analysis of variance with a classification criterion (ANOVA 1) was used for each of the parameters and for each of the tides (Sokal & Rohlf 1995; El Morhit et al. 2012).

Principal Component Analyses (PCA) was conducted with the physicochemical data, and given to group sampling stations according to their environmental variables (Coakes et al. 2006, Amani 2012, Kaniz Fatema et al. 2014, N'Guessan et al. 2015, Rakotondrabe et al. 2018).

Correspondence Factorial Analyses (CFA) were performed with two aims: 1 – to give a synthetic picture of the affinities between the different populations of microalgae (phytoplankton), 2 – to highlight the relationships/correspondences between the taxa and the stations of the estuary (Daget 1979, Matiatos et al. 2014). The method used, based on the log10 (maximum abundance + 1) matrix, has been shown to be the most valid and effective in terms of the breakdown and dispersion of the scatterplots for revealing the biotypic structure of estuaries (Dessier 1983, Lam Hoai et al. 1985, Jouffre et al. 1991, and Tilston et al. 2000).

3. Results

3.1. Physico-chemical characteristics

3.1.1. Range of variation of the physicochemical parameters

The physicochemical parameters variation of the water of the Kienké estuary is presented in Table 1.

3.1.2. Spatiotemporal variation of the physicochemical parameters

The level of the temporal variation of temperature, electrical conductivity, pH, salinity, dissolved oxygen, suspended particulate matter, nitrates, ammonium and phosphate in the Kienké river estuary are shown below (Figures 2, 3 and 4).

3.1.2.1. Temperature, Electrical Conductivity and pH

At low tide, the mean temperatures decrease slightly away from the sea to the upstream part of the estuary, from 27.64°C (K1) to 26.98°C (K4). During high tide, the lowest mean temperature (27.18°C) was observed at the K1 station, along with a wider distribution of temporal values (Figure 2a). The analysis of the variance of the two sea states does not reveal any significant difference between stations

Table 1

Level of variation of physicochemical parameters in the Kienké estuary in Cameroon during the study period

Variables	Units	Avg. ± SD	Med.	Min.	Max	N
Temp.	°C	27.39 ± 2.33	27.75	22.6	31	64
EC	mS cm^{-1}	16.56 ± 12.05	14.78	0.22	49.7	64
S	PSU	11.51 ± 8.47	8.75	0	29.32	64
pH		7.75 ± 0.82	7.97	6	8.86	64
DO	mg l^{-1}	45.8 ± 31.48	64.05	4.7	86.3	64
SPM		9.02 ± 8.14	8.75	0	38	64
NH_4^+		0.96 ± 0.56	0.9	0	2.7	64
NO_2^-		0.13 ± 0.25	0.01	0	1.5	64
NO_3^-		0.81 ± 0.77	0.6	0	4	64
PO_4^{3-}		0.56 ± 0.81	0.2	0	3.59	64

Min. (minimum); Max (maximum); Avg. (mean); Med. (median); SD (standard deviation); N (number of samples); PO_4^{3-} (Phosphate) ; NO_3^- (nitrate); NO_2^- (nitrite); NH_4^+ (ammonium); SPM (suspended Particulate Matter), pH (hydrogen potential); DO (dissolved oxygen); Sal (salinity); EC (electrical conductivity); Temp. (water temperature)

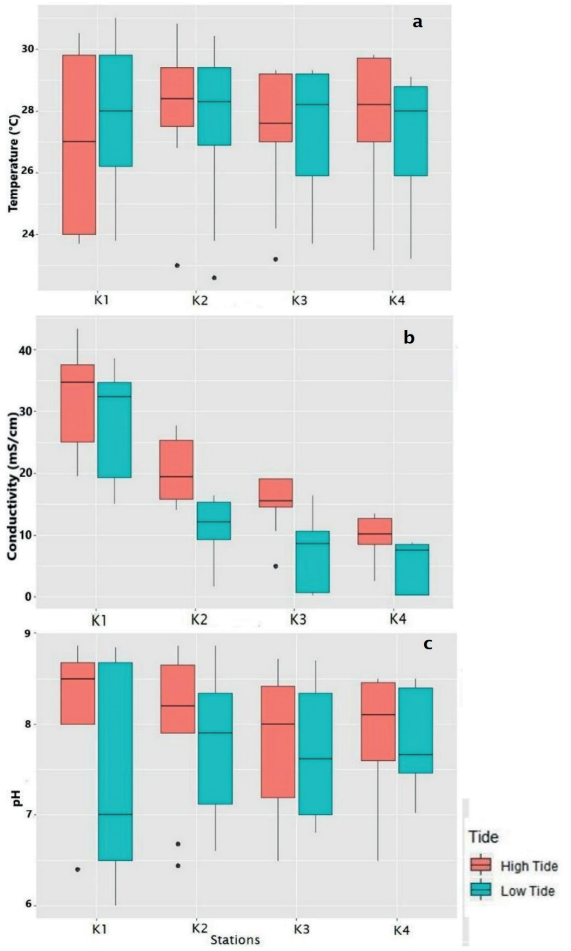

Figure 2

Level of temporal variation of : (a) water temperature, (b) water Electrical conductivity, (c) water pH in the Kienké estuary

($p > 0.05$). In the same way, the Student's t test reveals no significant intra-station difference in the effect of the tides ($p > 0.05$). The mean values of electrical conductivity evolve in a decreasing horizontal gradient downstream-upstream at low tide (29.94 to 6.19 mS cm^{-1}) and at high tide (33.50 to 14.06 mS cm^{-1}). The ANOVA 1 test on the spatial effect appears highly significant ($p < 0.0001$) during the sea water flow. From K2 to K4, the temporal variability shows a larger distribution during low tide compared to high tide. The amplitude of variability is lower at high tide and the spread of the boxes is less important, indicating a lower temporal fluctuation related to the sea water flow (Figure 2b). Conductivity varies significantly ($p < 0.05$) between the two tides at all stations except K1, where this difference is not significant. Fluctuations in pH are low during the flow of sea water into the estuary, and significant during the ebb tide (Figure 2c). Overall, the average pH values from downstream to upstream show relatively neutral water at low tide (7.47 to 7.80) and basic water at high tide (8.03 to 7.80). The spatial effect is highly significant during the flow (ANOVA 1, $p < 0.0001$). The tidal effect appeared to be not significant at each station (t-test, $p > 0.05$).

3.1.2.2. Salinity, Disolved Oxygen and Suspended Partuculed Matter

At a spatial level, the average salinity values at the different stations evolve in a decreasing manner from downstream to upstream. At low tide they range from 19.73% to 2.80% and at high tide from 25.01% to 5.92% (Figure 3a). The effect of the tide was highlighted by the Student's statistical test, which indicates a significant ($p < 0.05$) difference at points K1 and K2 and

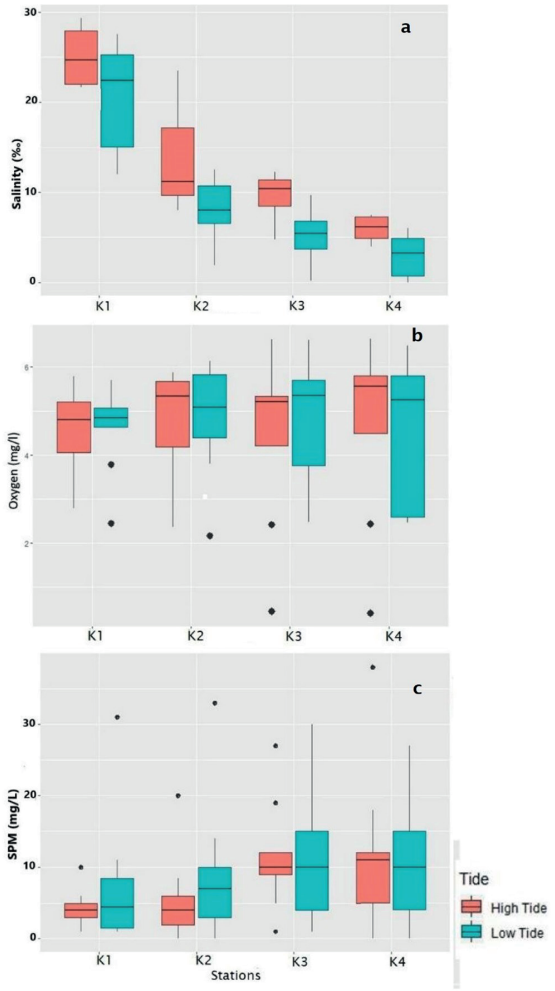

Figure 3

Level of temporal variation of: (a) water salinity, (b) water dissolved oxygen, (c) Suspended Particulate Matter in the Kienké estuary

highly significant ($p < 0.01$) at K3 and K4. The average dissolved oxygen values vary slightly from one point to another both at low tide (2.81 to 3.16 mg l^{-1}) and at high tide (3.41 to 4.12 mg l^{-1}). These values were below the medians. The range of the whiskers shown in the figure is spread out towards the minimum values, showing here that the measurements tend more towards the low values (Figure 3b). The ANOVA test shows high significant difference during the flow. The amplitude of the temporal variability is large at low tide.

During high tide, the distributions are smaller (K1, K2 and K3) indicating that SPM values vary little over time under the influence of sea water (Figure 3c). Overall, the average SPM values are higher upstream with 10.1 mg l^{-1} at K3 and 10.2 mg l^{-1} at K4 during low tide. Similarly, during high tide we observe 10.2 mg l^{-1} at K3 and 10.4 mg l^{-1} at K4. The Student's test does not reveal any difference between the stations according to the tide.

3.1.2.3. Nitrates, Ammonium and Phosphate

The nitrate average during high tide varied between 0.46 and 0.97 mg l^{-1}, while during low tide it was between 0.63 and 1.63 mg l^{-1} (Figure 4a). The box plots show during both tidal cycles the distributions of the temporal measurements tending towards above average values. During the low tide the temporal variability is low between points K2 and K3, while K4 shows the maximum value of 2.6 mg l^{-1}. Although the average concentration evolves in an increasing way from downstream to upstream, thus indicating a horizontal gradient due to the arrival of marine waters, the tidal effect appears to be insignificant (Student test, $p > 0.05$). On a spatial scale, points K2 and K4 show little temporal variability due to the narrowing of the boxes at low tide. It appears that during high tide the means of points K2 (0.88 mg l^{-1}), K3 (0.87 mg l^{-1}) and K4 (0.94 mg l^{-1}) are above the median values, with bins extended towards the larger ammonium measurements. Station K1 shows an ammonium depletion during the ebb tide of the order of 0.74 mg l^{-1} compared to 1.06 mg l^{-1} above the median (Figure 4b). The temporal variability appears to be very low at high tide, due to the tight shape of the boxes, reflecting a low dispersion of the phosphate values, despite the presence of several atypical values at each point that projects the means (0.50 to 0.83 mg l^{-1}) well above the medians (0.11 to 0.21 mg l^{-1}). During the ebb tide, a low temporal variability is observed at point K3, whereas K1 has a larger box, resulting in a greater temporal dispersion during the study (Figure 4c). A significant spatial effect is revealed during the ebb (ANOVA 1, $p < 0.05$).

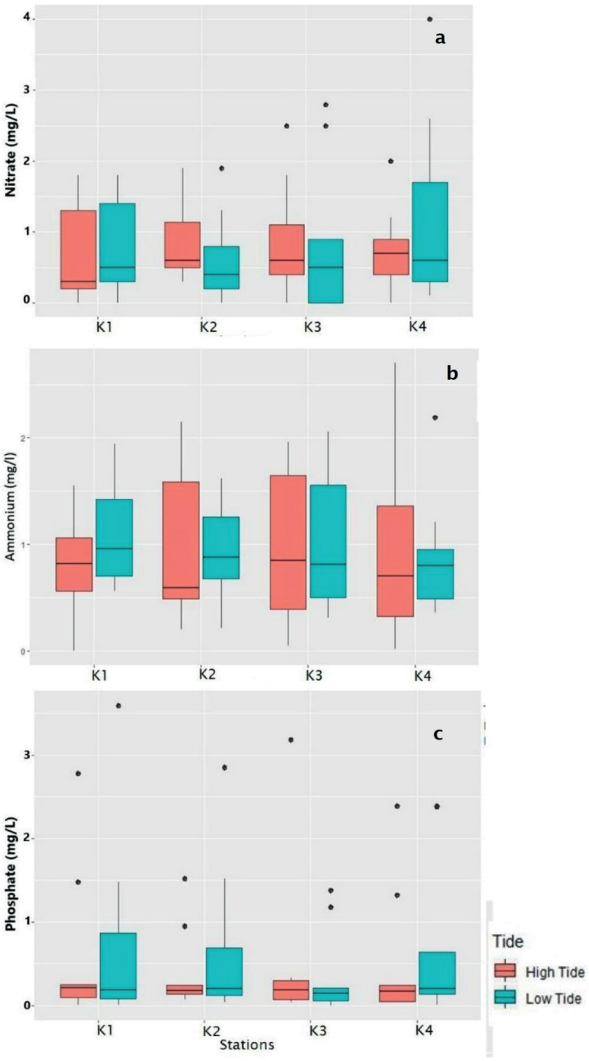

Figure 4

Level of temporal variation of: (a) nitrates, (b) ammonium, (c) phosphate in the Kienké estuary water

3.2. Phytoplankton characteristics of the waters in the Kienké estuary

3.2.1. Phytoplankton diversity of composition

A total of 167 taxa were identified and divided into five groups (Table 2). The Chrysophyta group is the most diversified with 4 classes, 10 orders, 17 families, 30 genera, and 60 species. It is followed by the Chlorophyta, Pyrrophyta, and Cyanophyta groups. The less diversified group is the Euglenophyta group with 1 class, 1 order, 2 families, 6 genera and 13 species.

Table 2

Global taxonomic richness of phytoplankton in the Kienké estuary

Division	Class	Orders	Family	Genus	Species	% of taxa
Chrysophyta	4	10	17	30	60	36.36
Chlorophyta	4	12	13	23	47	28.48
Cyanophyta	1	4	7	15	29	17.57
Pyrrophyta	2	4	7	9	16	9.70
Euglénophyta	1	1	2	6	13	7.87
Total	12	31	46	83	165	100

3.2.2. Specific richness

The Kienke estuary is characterised by the dominance of the class Diatomophyceae, which makes up 32% of the total species richness. It is followed by the classes Chlorophyceae (22%), Cyanophyceae (20%), Dinophyceae (10%), Euglenophyceae (7%) and Chrysophyceae (4%) (Figure 5).

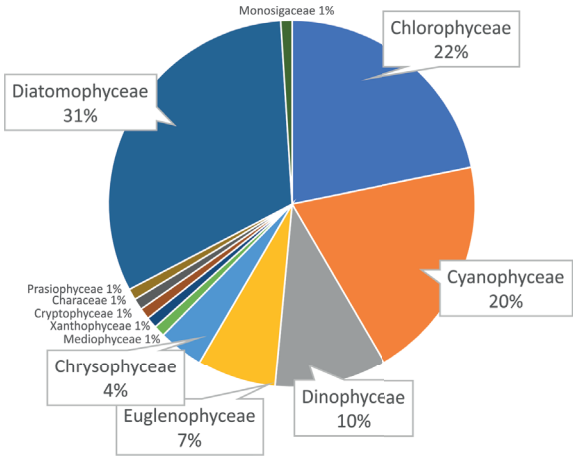

Figure 5

Biological spectrum defined according to phytoplankton classes

3.3. Spatiotemporal variations in the phytoplankton composition in the estuary waters

3.3.1. Relative abundance

At low tide, the Diatomophyceae class dominates the phytoplanktonic population of the estuary with 32%, followed by the Cyanophyceae class with 19%. During high tide, the Chlorophyceae dominate with 27% of the total abundance, followed by the Cyanophyceae with 22%. The Dinophyceae class increases from 7% during low tide to 10% during high tide (Figure 6a). The Chrysophyceae class is absent during high tide, but represents 3% during low tide (Figure 6b).

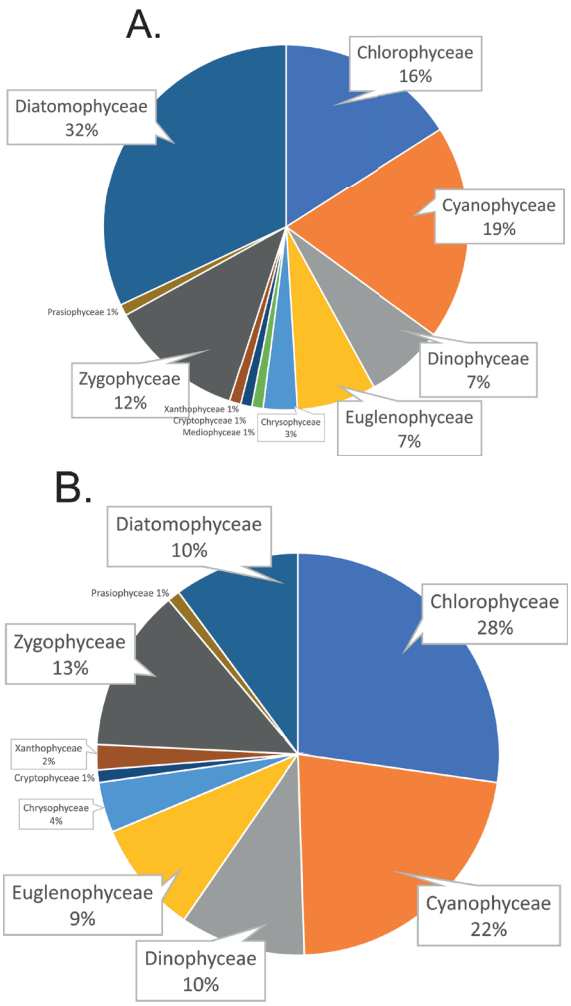

Figure 6

Variation of the biological spectrum of phytoplankton according to the tides (A: Low Tide; B: High Tide)

3.3.2. Spatial and tidal variation in total taxonomic richness and quality structure by algal classes

During low tide, point K3 is the richest with 53 species, followed by K1 with 52 species (Figure 7). It can be seen that at the downstream point K1, placed in the open sea, the class Diatomophyceae has 17 species, followed by Chlorophyceae (10 species), Cyanophyceae (6 species), and Dinophyceae (3 species) (Figure 8). At the K2 point, the classes Chlorophyceae and Diatomophyceae have 14 species each, followed by Cyanophyceae (12 species), Dinophyceae, (4 species) and Euglenophyceae (3 species). In K3, the dominant class is the Diatomophyceae with 19 taxa, followed by the Chlorophyceae (13 species). The species richness observed at the upstream point K4 is dominated by the class of Diatomophyceae with 13 species and that of Chlorophyceae (11 species).

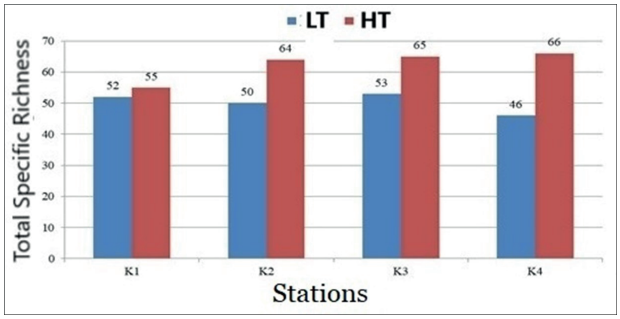

Figure 7

Spatial and tidal variation of the total specific richness in the Kienké estuary (low tide = LT; high tide = HT)

During high tide, points K2 (64 species), K3 (65 species), and K4 (66 species) are the richest (Figure 7). At K1, the Dinophyceae and Cyanophyceae classes each have 8 species (Figure 8). At K2, the Chlorophyceae and Diatomophyceae each consist of 14 species. They are followed by the Cyanophyceae with 12 species and the Dinophyceae (6 species). Point K3 is dominated by the Chlorophyceae with 20 species, followed by the Diatomophyceae (19 taxa) and Dinophyceae (2 species). At K4, the classes containing more taxa are Chlorophyceae (15 taxa), Cyanophyceae (16 taxa) and Diatomophyceae (13 taxa).

The Student's *t*-test reveals a highly significant difference at high tide ($p < 0.001$) at points K2, K3 and K4.

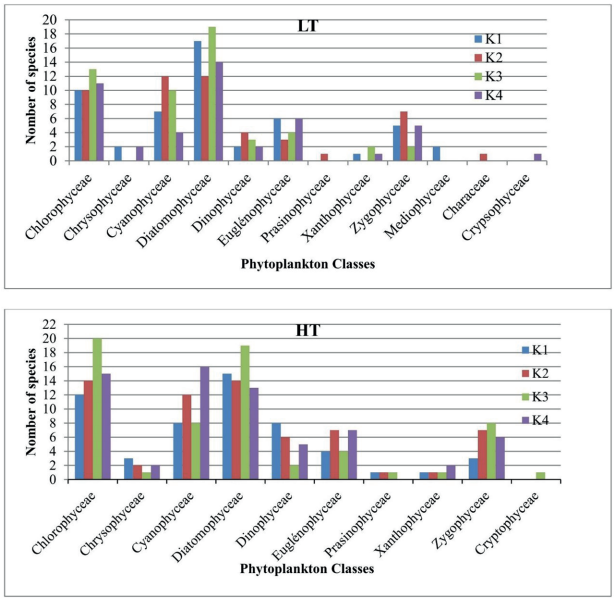

Figure 8

Specific richness by phytoplankton classes and sampling points (low tide = LT; high tide = HT)

3.4. Multivariate analysis

3.4.1. Principal component analysis of physicochemical parameters of the water during low tide

The examination of the correlation matrix between the variables during low tide reveals the presence of a first group of parameters that are correlated ($0.7 < r \leq 0.9$) to each other (Table 3). In this case, a significantly positive correlation was observed between electrical conductivity, salinity, and ammonium ions; between pH, dissolved oxygen and nitrite ions; between dissolved oxygen, suspended matter and nitrite ions, and between suspended matter and nitrate ions. A second group consists of variables with a medium correlation ($0.5 \leq r < 0.7$): between salinity and orthophosphate ions; between pH and suspended matter; between dissolved oxygen and nitrite ions, and between suspended matter and nitrite ions. Furthermore, significantly negative correlations ($r \geq -0.6$) were observed between the analysed parameters. These are: the correlations between temperature and nitrate ions; between electrical conductivity, pH, dissolved oxygen, and suspended matter and nitrite ions. In addition, a negative correlation is observed between: salinity and pH, dissolved oxygen and nitrite ions, pH with orthophosphate ions, dissolved oxygen and ammonium ions, then dissolved oxygen and orthophosphate, between ammonium and nitrite, and finally between nitrite and orthophosphate.

In the case of Principal Component Analysis (PCA), the first two principal components were taken into consideration due to the large proportion of the total variance they provide information on, i.e. 89.47%. The F1 axis contains 68.27% of information and the F2 axis contains 21.20% (Figure 9).

The organisation of the variables on the F1xF2 plane represented as a correlation circle revealed that the F1 axis is expressed towards its positive pole by salinity, electrical conductivity and ammonium ions. These variables contribute strongly to its formation at 0.99, 0.98, and 0.75 correlation respectively (Figure 9A). On the negative pole, it is expressed by the variables that are strongly and negatively correlated to it, namely pH (-0.96), dissolved oxygen (-0.95), SPM (-0.80) and nitrite ions (-0.96). On the other hand, the F2 axis is defined by temperature towards its positive pole with a correlation of 0.95. Nitrate and orthophosphate levels contribute to the formation of this axis towards the negative pole with a correlation of -0.73 and -0.69 respectively (Figure 9A).

The simultaneous representation of the sampling points and the abiotic variables reveals three groups

Table 3

Correlation matrix of physicochemical parameters during low tide

Variables		Temp.	EC	Sal.	pH	DO	SPM	NH_4^+	NO_2^-	NO_2^-	PO_4^{3-}
		°C	mS cm^{-1}	PSU		mg l^{-1}					
Temp.	°C	1									
EC	mS cm^{-1}	0.248	1								
Sal.	PSU	0.214	0.999	1							
pH		-0.134	-0.988	-0.995	1						
DO	mg l^{-1}	-0.106	-0.933	-0.923	0.904	1					
SPM		-0.525	-0.736	-0.699	0.629	0.835	1				
NH_4^+		0.306	0.813	0.831	-0.848	-0.553	-0.306	1			
NO_2^-		-0.069	-0.984	-0.989	0.994	0.939	0.655	-0.785	1		
NO_3^-		-0.899	-0.597	-0.561	0.481	0.526	0.832	-0.452	0.446	1	
PO_4^{3-}		-0.460	0.572	0.571	-0.583	-0.794	-0.511	0.092	-0.671	0.031	1

PO_4^{3-} (Phosphate); NO_3^- (nitrate); NO_2^- (nitrite); NH_4^+ (ammonium); SPM (Suspended Particulate Matter), pH (hydrogen potential); DO (Dissolved Oxygen); Sal. (Salinity); EC (Electrical Conductivity); Temp. (water temperature)

on either side of the PCA plane (Figure 9B). Group I in the downstream zone around K1 is characterised by salinity, ammonium content and electrical conductivity. Group II in the upstream zone around K3 and K4 is characterised by pH, dissolved oxygen, SPM, nitrate and nitrite levels. Group III consists of point K2 and is characterised by temperature (Figure 9B).

ammonium ions and nitrate ions. There are average correlations between the parameters ($0.5 \leq r \leq 0.7$), namely: the temperature with ammonium ions and nitrite ions; dissolved oxygen with SPM and nitrite ions; SPM with nitrate ions; ammonium ions and nitrite ions. Several other variables appear inversely correlated ($r > -0.6$).

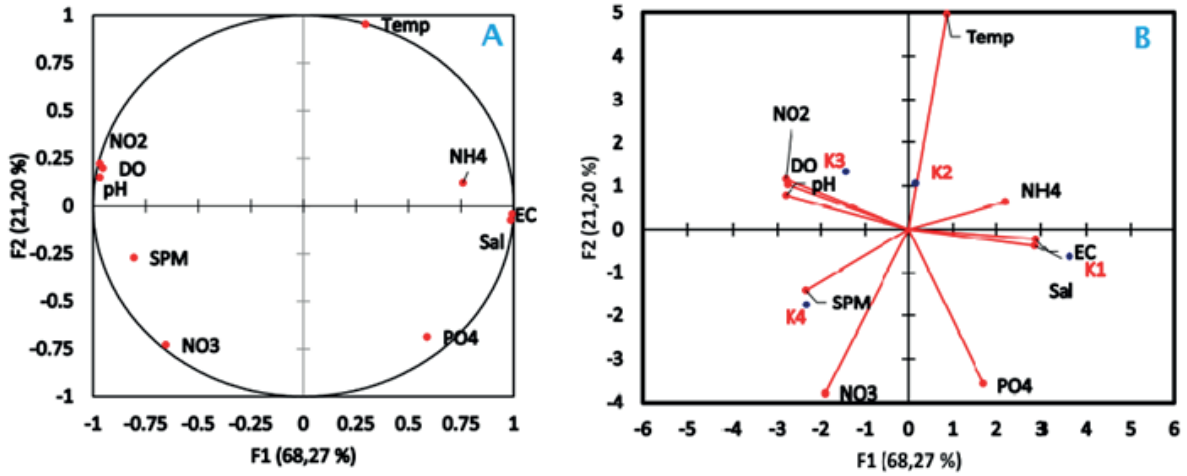

Figure 9

Correlation circle (A) and distribution of points with respect to their abiotic characteristics (B) in the F1 × F2 factorial plane of the PCA in the estuary during low tide

3.4.2. Principal component analysis of the physicochemical parameters of the water during high tide

The correlation matrix of physicochemical variables measured during high tide on the Kienké River shows a strong correlation between parameters ($r > 0.7$) (Table 4). Among others, strong positive correlations were found between: electrical conductivity, salinity and pH;

In the PCA design, the first two factorial axes (F1 and F2) express 87.92% of the total information during the study period at high tide (Figure 10). The F1 axis contributes 63.06% and is strongly correlated on its positive pole to salinity (0.98), electrical conductivity (0.97) and pH (0.79). At its negative pole, F1 is strongly correlated to SPM (-0.80), dissolved oxygen (-0.76), ammonium ions (-0.80), nitrites (-0.76) and nitrates (-0.79). The F2 axis expresses 24.86% of the total

Table 4

Correlation matrix of physicochemical parameters during high tide

Variables		Temp.	EC	Sal.	pH	DO	SPM	NH_4^+	NO_2^-	NO_2^-	PO_4^{3-}
		°C	mS cm^{-1}	PSU		mg l^{-1}					
Temp.	°C	1									
EC	mS cm^{-1}	-0.354	1								
Sal.	PSU	-0.403	0.997	1							
pH		0.064	0.907	0.878	1						
DO	mg l^{-1}	0.230	-0.846	-0.815	-0.846	1					
SPM		-0.078	-0.904	-0.881	-0.990	0.772	1				
NH_4^+		0.663	-0.687	-0.736	-0.386	0.247	0.456	1			
NO_2^-		0.790	-0.699	-0.708	-0.434	0.769	0.365	0.502	1		
NO_3^-		0.398	-0.724	-0.762	-0.532	0.246	0.621	0.950	0.312	1	
PO_4^{3-}		-0.903	0.417	0.479	0.008	-0.073	-0.053	-0.888	-0.585	-0.705	1

PO_4^{3-} (Phosphate); NO_3^- (nitrate); NO_2^- (nitrite); NH_4^+ (ammonium); SPM (Suspended Particulate Matter), pH (hydrogen potential); DO (Dissolved Oxygen); Sal. (Salinity); EC (Electrical Conductivity); Temp. (water temperature)

variance and is defined by temperature (-0.77) towards its negative pole. At its positive pole, the F2 axis is positively correlated by orthophosphate ions (0.79) (Figure 10.A).

The figure 10B shows the distribution of sampling points with their physicochemical characteristics. Three large groups of points emerge on this factorial plane. The F1 axis discriminates the K3 and K4 points (group I), characterised by dissolved oxygen, suspended solids, nitrate ions, nitrite ions and ammonium ions, in negative coordinates. The F1 axis also isolates, but in its positive part, point K1 (group II), characterised by salinity, electrical conductivity and pH. The F2 axis discriminates in negative coordinates the point K2 (group III), characterised by temperature, which opposes orthoposphate ions (Figure 10).

3.4.3. Correspondence Factor Analysis during low tide

The two binary matrices processed, at low and high tide, have 4 points × 71 taxa and 4 points × 74 taxa respectively. The correspondence between the row points (sampling points) and the column points (taxa) was sought in the flat graphical representations produced by a system of factorial axes.

The first two axes (F1 and F2) of the CFA design gives 78.37% of the information contained in the Kienké low tide baseline data table. F1 alone explains 42.44% of the total inertia. Point K2 on the positive pole of the first factorial axis contributes to its explanation with 56.80% of the total inertia, and on the negative pole K1 contributes 28.84% (Figure 11A).

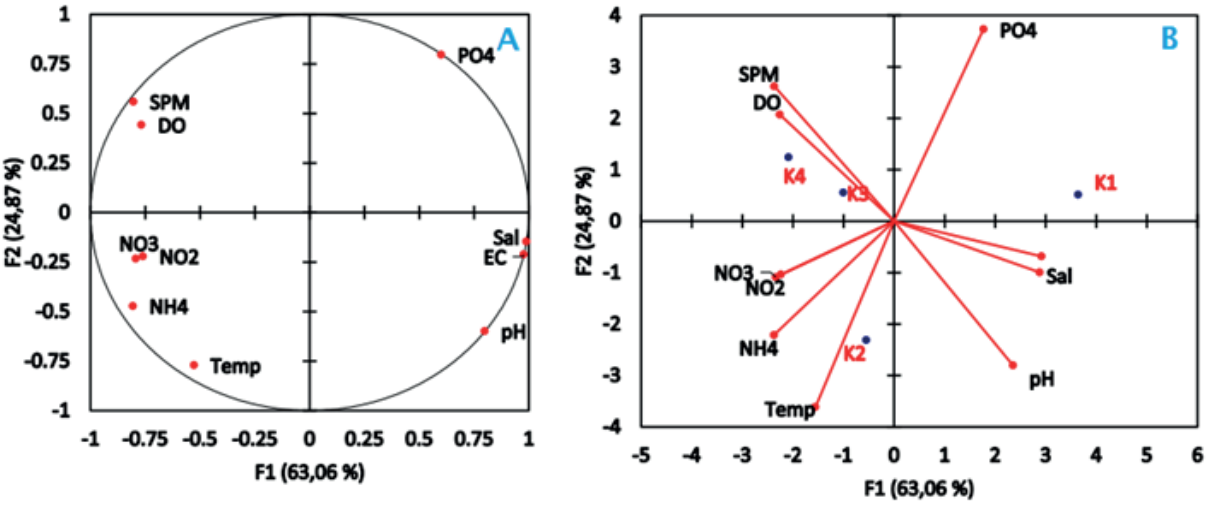

Figure 10

Correlation circle (A) and distribution of points with respect to their abiotic characteristics (B) in the F1 × F2 factorial plane of the PCA in the estuary during high tide

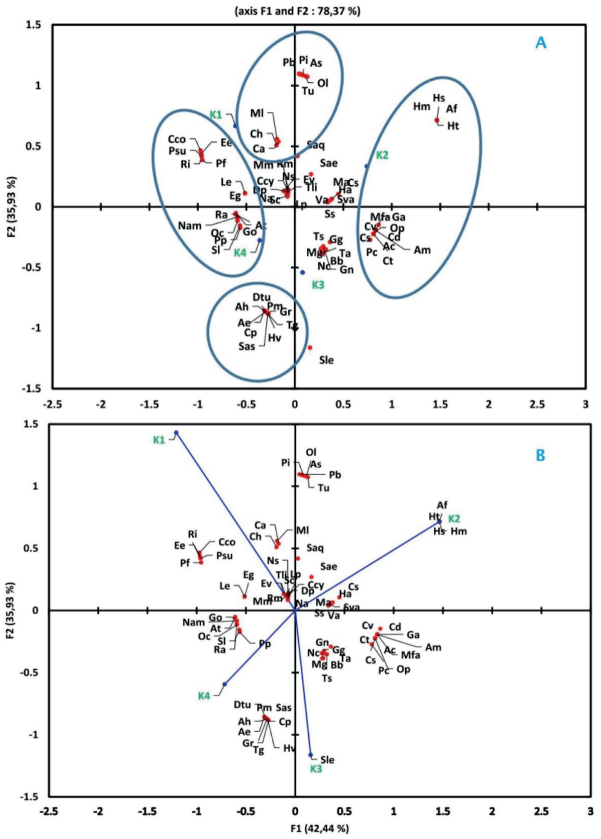

Figure 11

Graphical representation of inventoried taxa and sampling points (A) and asymmetric graph of the distribution of taxa in a sampling point space (B) in the F1 × F2 factorial plane of the CFA during low tide

The distribution of the scatterplot in the F1 × F2 factorial design shows 4 (four) groups on the F1 axis (Figure 11A). These clusters are made up of taxon items whose variance is strongly attributed to the F1 factor in the F1 × F2 CFA design. On the negative pole of F1, elements whose variance is due to F1 are : *Rivularia aquatica* (Ra), *Gomphonema olivaceum* (Go), *Astasia torta* (At), *Peridinium pusillum* (Pp), *Ophiocytium cochleare* (Oc), *Schizomeris leibleinii* (Sl), *Nitzschia amphibia* (Nam). This first group (group I) has well represented taxa ($Cos^2 \geq 0.8$) on F1. The second group (group II) *Phacus suecicus* (Psu), *Euglena ehrenbergii* (Ee), *Polyblepharides fragariiformis* (Pf) and *Rhizosolenia iongiseta* (Ri) has taxa also well represented ($cos^2 \approx 0.7$) but far from the origin. At the positive pole, the taxa related to this axis are respectively: *Hapalosiphon* sp. (Hs), *Hyalotheca mucosa* (Hm), *Anabaena flos-aquae* (Af), *Helicotheca tamesis* (Ht), (group III) with well-represented elements ($cos^2 \approx 0.7$) and far from the origin. Group IV is represented by taxa close to the origin and very well represented on F1, which are : *Arthrodesrnus mucronulatus* (Am), *Chroococcus turgidus* (Ct), *Amphidinium cucurbita* (Ac), *Ceratium declinatum* (Cd), *Gonatozygon aculeatum* (Ga), *Mougeotia floridana* (Mfa), *Chara vulgaris* (Cv), *Calothrix scytonemicola* (Cs) and *Peridinium cinctum* (Pc).

The F2 axis expresses 35.93% of the total inertia. On the positive pole is identified the group (V) made up of the following species: *Pediastrum boryanum* (Pb), *Phymatodocis irregulare* (Pi), *Ankistrodesmus* sp. (As), *Oocystis lacustri* (Ol), *Toxarium undulatum* (Tu), all having a $cos^2 > 0.90$. Related to this axis are the species *Microcoleus lacustris* (Ml), *Ceratium hirundinella* (Ch), and *Closterium aciculare* (Ca), with a representation having $cos^2\varepsilon$ [0.60; 0.75]. On the negative pole, the well represented taxa ($cos^2 > 0.80$) contribute well to the construction of the axis. Here are the species *Dichotomosiphon tuberosus* (Dtu), *Prorocentrum micans* (Pm), *Gymnodinium rofundatum* (Gr), *Tetraspora gelatinosa* (Tg), *Hemiselmis virescens* (Hv), *Closterium parvulum* (Cp), *Stephanodiscus astraea* (Sas), *Aphanothece elabens* (Ae), and *Actinastrum hantzschii* (Ah).

The distribution of taxa in the space of the sample points in the F1 × F2 plane of the CFA presented in Figure 11B illustrates a first dimension which opposes the point K4 to the point K2. In this dimension, the group of microalgae composed of the species *Hapalosiphon* sp. (Hs), *Hyalotheca mucosa* (Hm), *Anabaena flos-aquae* (Af), *Helicotheca tamesis* (Ht), and the group composed of the species *Hantzschia amphioxys* (Ha), *Calothrix scytonemicola* (Cs), *Microcystis aeruginosa* (Ma), *Sorastrum spinulosum* (Ss), *Volvox aureus* (Va), and *Staurodesmus validus* (Sva), are the most abundant at the point K2. The second dimension contrasts K3 and K1. The largest proportion of K3 is made up of the species: *Synechococcus leopoliensis* (Sle), *Prorocentrum micans* (Pm), *Stephanodiscus astraea* (Sas), *Closterium parvulum* (Cp), *Dichotomosiphon tuberosus* (Dtu), *Hemiselmis virescens* (Hv), *Tetraspora gelatinosa* (Tg), *Goniochloris gigas* (Gg), *Aphanothece elabens* (Ae), *Actinastrum hantzschii* (Ah). The largest proportion of point K1 comes from the taxa represented by the species: *Thalassiosira lineata* (Tli), *Surirella capronii* (Sc), *Lioloma pacificum* (Lp), *Dictyosphaerium pulchellum* (Dp), *Navicula* sp. (Na), *Raphidiopsis mediterranea* (Rm), *Mesotaenium macrococcum* (Mm) and *Euglena viridis* (Ev).

3.4.4. Correspondence Factorial Analysis during high tide

The projection onto the plane of the CFA formed by the F1 and F2 axes presents a representation of the

cloud of sampling points and taxa during high tide on the Kienké (Figure 12). These two axes represent 75.39% of the total variance at high tide, i.e. 43.78% for the F1 axis and 31.60% for F2. On the positive pole of the F1 factor, point K3 contributes relatively 72.06% to the formation of F1. On the positive pole of the F2 axis, the point K4 contributes 50.35% to the explanation of the axis. On the negative pole, K1 contributes 49.28% to the formation of this second axis.

From the F1 × F2 point cloud, we can see groups of taxa on either side of the F1 and F2 axes (Figure 12A). The F1 axis brings together at the negative pole group I composed of the following species: *Strombomonas verrucosa* (Sv), *Aphanothece elabens* (Ae), *Cladophora holsatica* (Cho), *Melosira granulata* (Mg), *Sphaeroeca volvox* (Svo), *Rivularia aquatica* (Ra), *Mougeotia floridana* (Mfl), *Colacium cyclopicola* (Ccy), *Hemidiscus cuneiformis* (Hc), *Micractinium pusillum* (Mp), and *Tetraedron muticum* (Tm) well represented with $\cos^2 = 0.9$. On the positive pole, we have group II where the species *Navicula* sp. (Na), *Coelosphaerium conferium* (Cco), *Sorastrum spinulosum* (Ss), *Cyclotella stelligera* (Cs) are related, and *Ankistrodesmus* sp. (As), *Volvox aureus* (Va), *Denticula thermalis* (Dt), *liemophora ehrenbergii* (Le), *Stigeoclonium aestivale* (Sa), and *Thalassionema frauenfeldii* (Tf), represented on the factor with $\cos^2 = 0.6$.

On the factorial axis F2, the positive pole is constituted by group III consisting of the following taxa: *Hapalosiphon* sp. (Hs), *Astasia torta* (At), *Actinastrum hantzschii* (Ah), and *Kirchneriella obesa* (Ko), with $0.6 \leq \cos^2 \leq 0.78$, which are well represented. On the negative pole of F2 the taxa best related to this axis are grouped in IV, consisting of the species: *Pleurotaenium trabecula* (Pt), *Oscillatoria platensis* (Op), *Spatulodinium* cf. *pseudonoctiluca* (Sp), *Closterium aciculare* (Ca), *Raphidiopsis mediterranea* (Rm) and then *Dichotomosiphon tuberosus* (Dtu), *Anabaenopsis arnoldii* (Aa), *Coelastrum microporum* (Cm), *Coscinodiscus excentricus* (Ce), *Dinobryon sertularia* (Ds), *Ceratium hirundinella* (Ch), *Binuclearia eriensis* (Be), *Anabaena flos-aquae* (Af), and *Noctiluca scintillans* (Nsc). All taxa related to this negative pole of the axis have cosine values such that $0.6 \leq \cos^2 \leq 0.78$ (Figure 12A).

On the asymmetrical graph of taxa in the space plane of the CFA sample points, a first dimension appears which opposes K3 and K2 (Figure 12.B). The clusters [*Hemidiscus cuneiformis* (Hc), *Micractinium pusillum* (Mp), *Tetraedron muticum* (Tm)], [*Navicula sp* (Na), *Coelosphaerium conferium* (Cco), *Sorastrum spinulosum* (Ss), *Cyclotella stelligera* (Cs), *Ankistrodesmus sp* (As), *Volvox aureus* (Va), *Denticula thermalis* (Dt), *Stigeoclonium aestivale* (Sa), and *Thalassionema frauenfeldii* (Tf)] have taxa that contribute to the

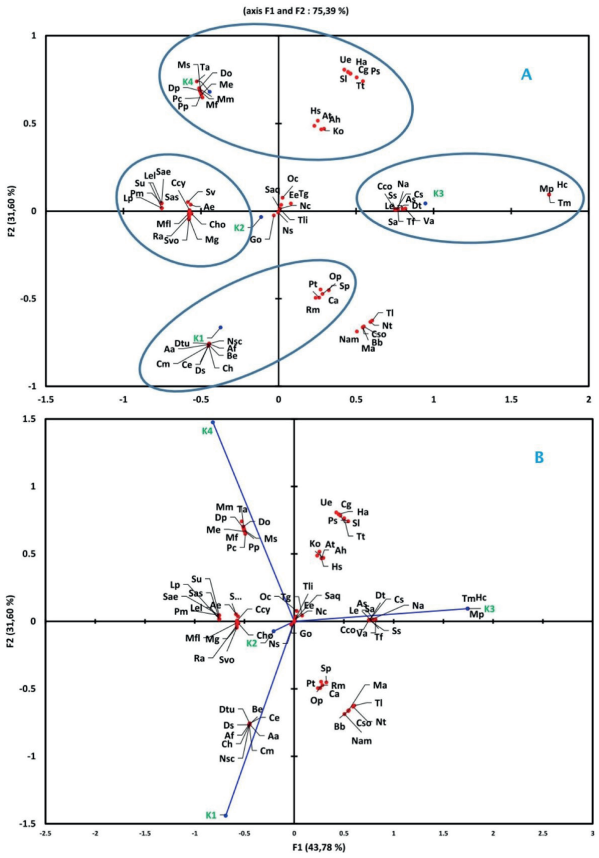

Figure 12

Graphical representation of inventoried taxa and sampling points (A) and asymmetric graph of the distribution of taxa in a sampling point space (B) in the F1 × F2 factorial plane of the CFA during high tide on the Kienké

construction of the K3axis. The first subgroup has taxa that contribute more, given their positions at the end of the axis. The second dimension contrasts K4 and K1. On K4, the phytoplankton assemblage *Mesotaenium macrococcum* (Mm), *Trentepohlia arborum* (Ta), *Diploneis ovalis* (Do), *Mastigocladus* sp. (Ms), *Peridinium pusillum* (Pp), *Peridinium cinctum* (Pc), *Micrasterias foliacea* (Mf), *Dictyosphaerium* and *Pulchellum* (Dp), have a larger proportion but are close to the origin. The subgroup [*Dichotomosiphon tuberosus* (Dtu), *Anabaenopsis arnoldii* (Aa), *Coelastrum microporum* (Cm), *Coscinodiscus excentricus* (Ce), *Dinobryon sertularia* (Ds), *Ceratium hirundinella* (Ch), *Binuclearia eriensis* (Be), *Anabaena flos-aquae* (Af), and *Noctiluca scintillans* (Nsc)] presents taxa with larger proportions for the constitution of K1, but all equally close to the origin.

4. Discussion

4.1. Spatial and temporal variations in the physicochemical parameters of the waters of the Kienké estuary

The level of temperature variation is related to the upstream-downstream extent of the estuary. The mean temperature of 27.39°C obtained in the Kienké estuary is typical of those obtained in other tropical and subtropical estuaries (Kaberi et al. 2012; Atanle et al. 2013; Davies & Ugwumba 2013; Mama et al. 2018). The temporal evolution at high tide is highly significant, a difference that would be justified by the fact that the measurements were carried out in a punctual way from one station to another and at irregular times sometimes when the sun was at its zenith along the estuary (Rossi 2008).

The arithmetic mean of the electrical conductivity of the waters of the Kienké estuary, which is higher than the median, reflects a greater mineralization due to the influence of the sea (tides, swells and waves) along the channel. The spatial effect is highly significant, with a difference of concentrations between upstream and downstream. This difference could be explained by the influence of the marine waters, which mineralise the estuaries (El Morhit et al. 2012). The tidal effect is significant in the majority of the Kienké points, except for K1. This could be justified by the influence of the sea flow which increases chloride ion concentrations in this part of the estuary (Fatema et al. 2014). This influence allows for a decreasing mineralization gradient from upstream to downstream and dilution by freshwater inputs from upstream.

The waters pH show low values (6) in the limnic domains and fairly high values (8.86) in the haline domains. The waters thus show a variable pH with probable fluctuations in salinity that follow the tidal cycle for basic waters and probably fluctuations in organic load for acidic waters. The mean pH is globally between 7.47 and 8.03 (alkaline) at all stations due to the buffering effect of the sea water. The shallow slope of the channel of the river port on the Kienké would justify the fact that the seawater dilutes the fresh water of the river up to the upstream limit where there is a waterfall. During high tide, the amplitude of pH variability is low in K1 and K2 due to the intrusion of sea water. A similar result was obtained by Sanaa (2006) showing that the low ranges of the whiskers are due to a minimisation of the pH fluctuations in time during the flow in the downstream part in contact with the sea water. On the other hand, in K3 and K4, the extent of the whiskers appears wide during the flow, indicating a strong fluctuation of the pH values in time due certainly due to the inflow of wastewater from the sewers of the military camp and the merchant navy which are close to K3, and also from the run-off water coming from the installations of the company CECOPAK. These domestic water intrusions tend to decrease the pH values.

Salinity is an important parameter in estuaries that varies according to the tidal range on one side and the river flow on the other. The Kienké estuary appears to be a mesohaline environment with an average of 11.51 PSU (McLusky 1981; DREAL 2013). The spatial effect was observed to be highly significant ($p < 0.01$) with respect to the tidal alternation. The presence of the cascade upstream of the harbour channel on the Kienké River makes the tide the main driver of the estuarine hydrodynamics at high tide where, during the flood currents, the mean salinity describes a decreasing downstream-upstream gradient from 25.01 PSU to 5.92 PSU. Although the amplitudes of variability are small at upstream points K2, K3 and K4, the salinity averages reveal a more significant temporal influence of seawater over the two tidal cycles. The difference due to the tide was found to be highly significant ($P<0.01$). A better homogeneity due to the mixing of the water during the flood is noticeable upstream of K1. Fluctuations in salinity as a function of river flow and tidal dynamics from downstream to upstream were also observed on Lake Noukoué in Benin (Mama 2010), and on the Sassandre estuary in Ivory Coast (N'Guessan 2015).

The percentage of dissolved oxygen saturation increases in the Kienké estuary during floods. This result is similar to those obtained in the Bou Regreg estuary (Mayif 1987; Cheggour 1988). The amplitudes of variability appear to be identical, with wide whiskers that reflect the strong temporal fluctuation of the oxygen.

SPM are generally low and range from 0 to 38 mg/l with an average of 9.09 ± 8.14 mg l^{-1}. The values observed are generally lower than those of the SPM obtained upstream of the coastal rivers south of the Sanaga in the forest zone (Ndam Ngoupayou 1997; Lienou 2007; Nkoue 2008) and on the Kienké at Kribi (Lienou 2007). These low SPM contents in the Kienké estuary waters are linked to the marine influence, which is a clogging and sedimentation factor in these environments (Avoine et al. 1985; El Morhit et al. 2012). The mean concentrations of SPM contained in the water increase from downstream to upstream during both low and high tides. This gradient was observed by Amzough (1999) in the Oum Er-rbia estuary in Morocco, and by Maia & Clavier (2000) in the Sinnamary estuary in French Guiana.

The upstream waters are more loaded due to faecal debris, degradation of the banks, plant debris and the resuspension of slowly settling fine sediments by the tidal currents (Gordon 1975; Baillie & Wels 1980). The abundance of phytoplankton upstream also favours SPM loading. Indeed, phytoplankton represents a significant part of the native SPM in tropical estuaries (Gobin 1987). The morphology of the river bed with the presence of a waterfall and riprap that creates significant turbulence during the circulation of water upstream of the estuary, could also be responsible for this high SPM load.

Nutrient salts are elements used for assessing the state and functioning of the environment over time. Nitrogen in its ammonium, nitrite, nitrate and phosphorus forms were analysed in this study.

Nitrogenous nitrogen levels were lower downstream than upstream due to the dilution factor of the sea and the oxygenation of the water These favour the oxidation of nitrites into nitrates. The flow current moves the pollutant load upstream, combined with the suspension of organic matter by the turbulence of the environment.

Nitrate levels in the Kienké estuary are low during both tidal cycles (4 mg l^{-1} and 2.5 mg l^{-1}). They are far from the levels obtained in some of Cameroon's estuaries, notably the Moungo and Douala estuaries, where they are of the order of 11 mg l^{-1}, inherent to more significant domestic and industrial inputs or even leaching from cultivated soils (Fonge et al. 2012).

Waters rich in organic matter are characterised by high levels of ammoniacal nitrogen, which represents the product of their degradation. This form of nitrogen is preferentially assimilated by phytoplankton compared to nitrates (Berman et al. 1984). The Kienké estuary benefits, in addition to the fluvial input from the upper river, from enrichment by wastewater runoff in the lower part of the estuary, which crosses the town of Kribi. This is in addition to the wastewater effluents from the restoration activities on the right bank of the estuary. A similar result was observed in the Douala estuary in Cameroon (Fonge et al. 2013).

The significant tidal effect on phosphorus averages calculated on the Kienké is remarkable for the weak distribution from upstream to downstream due to the stabilising capacity of the marine water introduced by the flow (Chambers & Odum 1990; Sanaa 2006). The input of orthophosphate ions into the environment is due to the leaching of the crossed soils, the decomposition of organic matter, and the phosphates which can come from the car wash in the car parks of the military camp and the administrative campus of the autonomous port of Kribi, all on the left bank of the estuary.

4.2. Spatiotemporal variations of phytoplankton in the waters of the Kienké estuary

The aim was to analyse variations in space and time in the taxonomic composition and structuring of the phytoplankton taxa identified in the Kienké estuary.

The Kienké estuary ecosystem, with 167 taxa, remains less diverse overall compared to the results of Sanaa (2006) on the Bou Regreg estuary in Morroco, where 307 taxa were collected, and Akoma's (2008) in the Imo River estuary in Nigeria, where 221 taxa were collected. However, the floristic list identified on the Kienke cannot be considered exhaustive.

Of the 5 groups of microalgae identified in all samples collected in this work, the Chrysophyta and Chlorophyta groups were the most abundant in the Kienké estuary (36.36% and 28.42%, respectively). This predominance is similar to results obtained in other tropical estuarine environments (Akoma 2008; Okosisi et al. 2012; Fonge et al. 2013; Mama et al. 2016; Mama et al. 2018). This predominance denotes the ability to survive and reproduce in a brackish and turbulent environment although chlorophyta, freshwater green algae, are less tolerant to salinity (Opute 2000).

The classes Diatomophyceae and Chlorophyceae were the most prominent in this ecosystem. Diatomophyceae led the way with 32% of the total species richness. The Diatomophyceae and Clorophyceae are globally heterogeneous classes of microalgae with species represented in all stations. This result corroborates those of some authors in estuarine ecosystems such as the Bou Regreg estuary (Sanaa 2006), Sundarbans (Suman et al. 2012) and Bahia Blanca (Arias et al. 2012).

In the Kienké estuary, the effect of the rising tide increases the number of Dinophyceae cells on the detriment of the other classes of microalgae, except for the Diatomophyceae, which always retain the upper hand during high tide. The qualitative predominance of the Diatomophyceae at high and low tide depend on the genus Amphora, Cocconeis, Licmophora and Nitzschia. The shallow depth of the estuary is the reason for this. It facilitates the resuspension of the sediment and the microphytobenthos it harbours (Tolomio et al. 1992; Mama et al. 2016).

From the point of view of habitat type affinity, in the Kienké estuary, exclusively marine taxa dominate downstream. Species indifferent to habitat type are distributed throughout the study site. The total species richness increases from downstream to upstream during high tide. The water of the sea flow suspends the benthic and terrestrial organisms found in the upstream sector of the study area. This is an open area at low tide where anthropogenic activities are likely

to enrich the environment with organic matter that favours the proliferation of micro-algae.

The distribution, composition and diversity of phytoplankton organisms in the Kienké estuary are influenced by the nutrient concentrations, location and the physical nature of the environment. This has an impact on the quality of the ecosystem (Reid 1961; Fonge et al. 2012).

4.3. Physicochemical functioning of the estuary

In the Kienké estuary, strong correlations are observed between some physicochemical variables (salinity, conductivity, pH and ammonium ions) during low and high tide indicating that the evolution of the latter is driven by the process of marine water intrusion into the river. This result is similar to that found in the Merbock estuary in Malaysia (Muduli et al. 2011; Kaniz-Fatema et al. 2014). The PCAs conducted in the Kienké estuary during the flood and ebb tides show sampling points that are distributed along the F1 factorial axis. This distribution shows that during low tide, salinity, conductivity and ammonium are opposite to the pH, dissolved oxygen, nitrite and SS. The arrangement of the points on the factorial plane reflects a hierarchical progression from upstream to downstream of the river channel of the Kienké harbour. The F1 axis defines a mineralization gradient, or enrichment in dissolved salts, from the positive pole to the negative pole. The negative correlation between this first factorial axis and the elements grouped at the negative pole reflects an enrichment in organic matter and nutrient salts. This organic matter could be linked to the pollutant load due to anthropic activities on both sides of the river, which would be responsible for the acidic trend of the waters upstream (Bhat et al. 2015; Kokoette & Aniefiok 2016).

The negative correlation between dissolved oxygen and the principal component, F1, during low and high tide indicates a state of pollution in the upstream sector of the study site. On the other hand, during ebb tide, point K4, which contributes more to the construction of the factorial axis F2 of the PCA, becomes individualised. This factorial is essentially determined by the temperature on the positive pole and nitrate and orthophosphate ions on the negative pole. During the flow, the F2 axis is determined by temperature, this time on the negative pole, and orthophosphate ions on the positive pole. These parameters evolve in opposite directions each time. This is because the temperature rise is spatial and not temporal and therefore varies from place to place. Under marine influence, the river temperature decreases, while the SPM, and the orthophosphate content, increase due to current and wave movement phenomena (Rossi 2008).

4.4. Interaction between the biological compartment and the physical and chemical conditions of the estuary

The qualitative composition of microalgae depends on the physicochemical characteristics of the water. The sub-groups of micro-algae are constituted according to the adaptation to the characteristics of the environment. At low tide on the Kienké, we find on the negative side of the F1 factorial axis in the F1 × F2 plane of the CFA, the subgroup made up of *Phacus suecicus* (Psu), *Euglena ehrenbergii* (Ee), *Polyblepharides fragariiformis* (Pf) and *Rhizosolenia iongiseta* (Ri) These taxa are fresh water taxa that adapt to salt water. Belonging to the same factorial plane as K4 and K1, they would have been transported downstream by the river current. According to Gupta (2009), these taxa proliferate in brackish and chlorinated waters of estuaries.

The Ee and Pf species are species that proliferate in environments rich in organic matter and sometimes they are able to adapt to oligotrophic environments (Alves-da-Silva & Menezes 2010). The subgroup containing the species *Gomphonema olivaceum* (Go, freshwater diatom), *Nitzschia amphibia* (Nam, freshwater and brackish diatom tolerant of high organic pollution), *Peridinium pusillum* (Pp, freshwater dynophyta), and *Schizomeris leibleinii* (Sl, freshwater chlorophyta) were grouped around the origin of the axes, showing that they can be found everywhere in the channel of the Kienké harbour.

The clustering of these taxa is similar to the results of Issifou et al. (2014) in coastal rivers of Togo. On the positive side of F1, the dominant subgroup consists of the species *Hapalosiphon* sp. (Hs), *Hyalotheca mucosa* (Hm), *Anabaena flos-aquae* (Af), *Helicotheca tamesis* (Ht), and the Cyanophyta (*anabaena flos-aquae* and *Hapalosiphon* sp.). This could be justified by their ability to tolerate variations in salinity and organic pollution (Rachana & Meenakshi 2016). The second subgroup, the Dinophyta species (*Amphidinium cucurbita*, *Ceratium declinatum*), taxa of marine waters, and Chlorophyta (*Gonatozygon aculeatum*) and Cyanophyta (*Chroococcus turgidus*), taxa of brackish waters, were found throughout the estuary. These microalgae prefer environments rich in dissolved salts, oxygenated and basic waters (Fernando Gomez 2005).

On the negative pole of the F2 factor are gathered the taxa from the K4 and K3 sampling points. These microalgae consist of marine species such as *Gymnodinium rotundatum* (Gr), *Hemiselmis virescens*

(Hv), and *Prorocentrum micans* (Pm) that can live in freshwater (Steidinger & Tangen 1996; Issifou et al. 2014; Yuri 2014). In this assemblage are freshwater but benthic species such as *Dichotomosiphon Tuberosur* (Dtu), *Aphanothece elebens* (Ae), and *Closterium parvulum* (Cp). According to Kadiri (1999), these taxa characterise environments rich in organic matter and nutritive salts. On the positive pole of axis F2 we have taxa from points K1 and K2 consisting of species such as *Phymatodocis irregulare* (Pi) and *Toxarium undulatum* (Tu), which are marine species tolerant of low pH and that can be found in shallow depths (Dembowska et al. 2018).

During high tide in the Kienké estuary, due to the rising tidal current, point K3 receives the same taxa as observed at stations K1 and K2 during low tide. The scatterplot of taxa in the F1 × F2 CFA planes indicates some floristic heterogeneity in the waters at K1, K2 and K3.

The floristic groups on the positive pole of F1 in the F1 × F2 plane include freshwater, brackish and marine taxa. Amongst others, freshwater taxa such as *Micractinium pusillum* (Mp) and *Tetraedron muticum* (Tm) of the Chlorophyta group have been identified. There are also marine species such as *Hemidiscus cuneiformis* (Hc) which arrived in the rising waters of the flood. The coexistence of these microalgae has been observed in the estuary due to the ability of Chlorophyta green algae to adapt to turbid waters and also their ability to use organic matter (Bouarab et al. 2004; Costa et al. 2009; Barroso et al. 2017). The subgroup consisting of Diatoms (*Denticula thermalis* (Dt), *Navicula* sp. (Na), *Cyclotella stelligera* (Cs)), Chlorophyta (*Coelosphaerium conferium* (Cco), *Sorastrum spinulosum* (Ss), *Ankistrodesmus* sp. (As), *Volvox aureus* (Va), *Stigeoclonium aestivale* (Sa), *Thalassionema frauenfeldii* (Tf)), and all freshwater species, is characterised by high salinity tolerance (Compère & Riaux-Gobin 2009). The taxon assemblage on the negative pole of F1 is composed of a mixture of Chrysophyta, Chlorophyta and Euglenophyta. These taxonomic groups preferentially contain freshwater and benthic species.

The assemblage of taxa on the negative pole of the F2 axis consists of the subgroup comprising the freshwater Cyanophyta (*Oscillatoria platensis* (Op)), the freshwater Charophyta (*Pleurotaenium trabecula* (Pt)), the Dinophyta (*Spatulodinium* cf. *pseudonoctiluca* (Sp)), and the Chrysophyta (*Closterium aciculare* (Ca)). The subgroup consisting of *Dichotomosiphon tuberosus* (Dtu), *Anabaenopsis arnoldii* (Aa), *Coelastrum microporum* (Cm), *Coscinodiscus excentricus* (Ce), *Dinobryon sertularia* (Ds), *Ceratium hirundinella* (Ch), *Binuclearia eriensis* (Be), *Anabaena flos-aquae* (Af), and *Noctiluca scintillans* (Nsc), includes species that are mostly microalgae of tropical rivers that can tolerate organic pollution and adapt to environmental fluctuations (Kiorboe & Tetelman 1998).

The subgroup of taxa on the positive pole of F2 includes microalgae from the Chlorophyta division (*Hapalosiphon* sp. (Hs), *Actinastrum hantzschii* (Ah), and *Kirchneriella obesa* (Ko)) and the Euglenophyta division (*Astasia torta* (At)). These are the freshwater taxa, indicative of organic pollution and likely to tolerate the enrichment in dissolved salts observable in intertidal waters such as estuaries and lagoons (Nwankwo 1996; Kokoette & Aniefiok 2016). The positive pole subgroup includes the freshwater blue and brown algae *Dictyosphaerium pulchellum* (Dp), *Micrasterias foliacea* (Mf), *Mastigocladus* sp. (Ms), *Trentepohlia arborum* (Ta), *Diploneis ovalis* (Do), *Mesotaenium macrococcum* (Mm), *Peridinium pusillum* (Pp), and *Merismopedia elegans* (Me). These are species that fix nitrogen in the presence of light, and they were collected in the K4 well oxygenated environment (Houssou et al. 2016).

The floristic assemblages in the F1 × F2 factorial designs from the Kienké data matrix during high tide are made up of taxa that contribute to the formation of the factorial axes and are more or less well represented on these main axes. The asymmetric plots of taxon distribution in the sample point plane illustrate the distance and relationship between taxa in different subgroups.

5. Conclusion

The Kienké estuary in Cameroon is characterized by instability and spatio-temporal variations of physicochemical parameters. Nutrients (ammonium, nitrites, nitrates and orthophosphates) vary very little in terms of space and time. They are relatively low in both estuaries with a longitudinal distribution that is controlled by the tidal flows, river flows and the biological pump. This estuary is characterized by a relatively rich and diverse taxonomic composition that varies in space and time and according to the tides. The cohabitation of taxa reveals eutrophic estuarine waters in the points located in the upstream part, and oligotrophic in the points located downstream. This structuring shows that the upstream areas are enriched with nitrogen from river inputs and the decomposition of organic matter, while the downstream areas, where salinization makes light available in the water column, contain species that tolerate a certain rate of nutrient poverty. The environmental factors that control the hydrobiogeochemical functioning of the Kienké

estuary are mainly represented by ocean and river dynamics and human activities.

Acknowledgments

This research article is the result of a strong collaboration between scientific researchers and technical stakeholders of the specialized Center for Marine Ecosystems Research (CERECOMA) and the University of Douala, Institute of Fisheries and Aquatic Sciences at Yabassi. Our special thanks also go to all the students who contributed to the realization of this document as well as independent researchers of Association of Professionals in Coastal and Aquatics Management (APCAM).

References

Akoma, O. C. (2008). Phytoplankton and Nutrient Dynamics of a Tropical Estuarine System, Imo River Estuary, Nigeria. *African Research Review, 2*(2), 253–264. https://doi.org/10.4314/afrrev.v2i2.41053

Alves-da-Silva, S. M., & Menezes, M. (2010). Eugleophyceae. In: Catálogo de plantas e fungos do Brasil. Rio de Janeiro: Andrea Jakobsson Estúdio; Instituto de Pesquisas Jardim Botânico do Rio de Janeiro. Vol.1, pp. 383-404.

Aminot, A., & Chaussepied, M. (1983). Manuel des analyses chimiques en milieu marin. Centre national pour l'exploitation des océans, 395 p. ISBN : 2.902721.10.2.

Amzough, M. (1999). Etude de l'évolution des paramètres physico-chimiques et biologiques dans l'estuaire du Bou Regreg. Mémoire de 3ème cycle, Institut Agronomique et Vétérinaire Hassan II, Rabat, Maroc.

Aye, B. A., Sababa, E., & Ndjigui, P. D. (2017). Geochemistry of S, Cu, Ni, Cr and Au-PGE in the garnet amphibolites from the Akom II area in the Archaean Congo Craton, Southern Cameroon. *Chemie der Erde, 77*(1), 81–93. https://doi.org/10.1016/j.chemer.2017.01.009

APHA. (2005). Standard methods for the examination of water and waste water (21st ed.). American Public Health Association.

Arias, A. H., Piccolo, M. C., Spetter, C. V., Freije, R. H., & Marcovecchio, J. E. (2012). Lessons From Multi-decadal Oceanographic Monitoring at an Estuarine Ecosystem in Argentina. Int. J. Environ. Res. 6(1): 219-234, ISSN: 1735-6865.

Atanle, K., Bawa, L. M., Kokou, K., Djaneye-Boundjou, G., & Edorh, M. T. (2013). Distribution saisonnière du phytoplancton en fonction des caractéristiques physico-chimiques du lac de Zowla (Lac Boko) dans le Sud- Est du Togo : cas de la petite saison sèche et de la grande saison sèche. Journal of Applied Biosciences. 64(3): 4847 – 4857, ISSN 1997–5902.

Avoine, J., Dubrulle, L., & Larsonneur, C. (1985). Dynamique sédimentaire dans les estuaires de la Baie de Seine - conséquences sur l'environnement. La Baie de Seine (GRECO-MANCHE) - Université de Caen, 24-26 avril 1985 IFREMER. *Actes de Colloques., 16*(4), 183–192.

Baillie, P. W., & Welsh, B. L. (1980). The effect of tidal resuspension on the distribution of intertidal epipelic algae in an estuary. *Estuarine and Coastal Marine Science, 10*(2), 165–180. https://doi.org/10.1016/S0302-3524(80)80056-9

Bakan, G., Özkoç, H. B., Tülek, S., & Cüce, H. (2010). Integrated environmental quality assessment of Kizihrmak river and its coastal environment. *Turkish Journal of Fisheries and Aquatic Sciences, 10*(1), 453–462.

Barroso, H. D. S., Santos, J. A., Marins, R. V., & De Lacerda, L. D. (2017). Assessing temporal and spatial variability of phytoplankton composition in a large reservoir in the Brazilian northeastern region under intense drought conditions. *Journal of Limnology, 77*. Advance online publication. https://doi.org/10.4081/jlimnol.2017.1698

Berman, T., Sherr, B. F., Sheer, E., Wynne, D., & Mccarthy, J. J. (1984). The characteristics of ammonium and nitrate uptake by phytoplankton in lake Kinneret. *Limnology and Oceanography, 29*(1), 287–297. https://doi.org/10.4319/lo.1984.29.2.0287

Beyene, A., Addis, T., Kifle, D., Legesse, W., Kloos, H., & Triest, L. (2009). Comparative study of diatoms and macro-invertebrates as indicators of severe water pollution: Case study of the Kabena and Akaki rivers in Addis Abeba, Ethiopia. *Ecological Indicators, 9*(2), 381–392. https://doi.org/10.1016/j.ecolind.2008.05.001

Ahmad Bhat, N., Wanganeo, A., & Raina, R. (2015). Variability in Water Quality and Phytoplankton Community during Dry and Wet Periods in the Tropical Wetland, Bhopal, India. *Journal of Ecosystem & Ecography, 5*, 160. https://doi.org/10.4172/2157-7625.1000160

Blandin, P. (1986). Bioindicateurs et diagnostic des systèmes écologiques. *Bulletin d'Ecologie., 17*(4), 215–307. ISSN: 0395-7217

Botes, L. (2001). Phytoplankton Identification Catalogue in Saldanha Bay, South Africa, GloBallast Monograph Series. 7: 88. IMO London. ISSN 1680-3078.

Bouarab, L., Dauta, A., & Loudiki, M. (2004). Heterotrophic and mixotrophic growth of Micractinium pusillum Fresenius in the presence of acetate and glucose: Effect of light and acetate gradient concentration. *Water Research, 38(11)*, 2706–2712. https://doi.org/10.1016/j.watres.2004.03.021 PMID:15207601

BUCREP. (2010). Etat et structures de la population : indicateurs démographiques. Rapport, 49p. Bureau Central de Recensement et d'Etude de la population au Cameroun.

Carmelo, R. (1997). Identifying Marine Phytoplankton. ISBN: 9780080534428

Casé, M., Leça, E. E., Leitão, S. N., Sant Anna, E. E., Schwamborn, R., & de Moraes Junior, A. T. (2008). Plankton community as an indicator of water quality in tropical shrimp culture

ponds. *Marine Pollution Bulletin, 56*(7), 1343–1352. https://doi.org/10.1016/j.marpolbul.2008.02.008 PMID:18538353

Cereja, R., Brotas, V., Cruz, J. P. C., Rodrigues, M., & Brito, A. C. (2021). Tidal and Physicochemical Effects on Phytoplankton Community Variability at Tagus Estuary (Portugal). *Frontiers in Marine Science, 8*, 675699, 21p. https://doi.org/10.3389/fmars.2021.675699

Cereja, R., Chainho, P., Brotas, V., Cruz, J. P. C., Sent, G., Rodrigues, M., Carvalho, F., Cabral, S., & Brito, A. C. (2022). Spatial Variability of Physicochemical Parameters and Phytoplankton at the Tagus Estuary (Portugal). *Sustainability (Basel), 14(20)*, 13324, 22p. https://doi.org/10.3390/su142013324

Chambers, R. M., & Odum, W. E. (1990). Pore water oxidation, dissolved phosphate and the iron curtain: Iron-phosphorus relations in tidal freshwater marshes. *Biogeochemistry, 10*, 37–52. https://doi.org/10.1007/BF00000891

Cheggour, M. (1988). Contribution à l'étude d'un milieu paralique : l'estuaire du Bou Regreg (côte atlantique marocaine). Conditions écologiques globales. Etude de la contamination métallique. Thèse de 3 ème cycle. Ecole Normale Supérieure Takaddoum, Rabat, Maroc. 337 p.

Coakes, J. S., Steed, L., & Dzidic, P. (2006). SPSS version 13.0 for Windows: Analysis without anguish. John Wiley and Sons Ltd.

Compère, P., & Riaux-Gobin, C. (2009). Diatomées de quelques biotopes marins, saumâtres et dulçaquicoles de Guinée (Afriqueo ccidentale). *Systematics and Geography of Plants, 79*(1), 33–66. https://doi.org/10.2307/20649771

Costa, L., Huszar, V., & Ovalle, A. (2009). Phytoplankton functional groups in a tropical estuary: Hydrological control and nutrient limitation. *Estuaries and Coasts, 32*(3), 508–521. https://doi.org/10.1007/s12237-009-9142-3

Crosnier. (1964). Fonds de pêche le long des côtes de la République Fédérale du Cameroun. Cah. ORSTOM, 133p.

Daget, J. (1979). Les modèles mathématiques en écologie. Ed. Masson, Paris, 172 p. ISBN/ISSN/EAN: 2-22544055-7

Davies, O. A., & Ugwumba, O. A. (2013). Tidal Influence on Nutrients Status and Phytoplankton Population of Okpoka Creek, Upper Bonny Estuary, Nigeria. *Journal of Marine Biology, 684739*, 16p. https://doi.org/10.1155/2013/684739

Dembowska, E. A., Mieszczankin, T., & Napiórkowski, P. (2018). Changes of the phytoplankton community as symptoms of deterioration of water quality in a shallow lake. *Environmental Monitoring and Assessment, 190*(2), 95. https://doi.org/10.1007/s10661-018-6465-1 PMID:29372414

Dessier, A. (1983). Variabilités spatiale et saisonnière des peuplements épiplanctoniques des copépodes du Pacifique tropical sud et équatorial (Est-Pacifique). *Oceanologica Acta, 6*(1), 80–103.

Djama, T. (1992). Interaction between the artisanal and industrial fisheries in Cameroun. pH.D Thesis University of Wales UK.

Djama, T. (1994). Analyse des éco-systèmes marins et côtiers de la Province du Sud. Projet CMR/92/008, 30p.

DREAL. (2013). Réseau des estuaires bretons – Qualité des eaux : Présentation et analyses des résultats – Campagne 2012, 182p. Direction Régionale de l'Environnement, de l'Aménagement et du Logement

Ducotroy, J. M., Mazik, K., & Elliott, M. (2016). Bio-sedimentary indicators for estuaries. *UOF, Paris., 4*(1), 1–16.

Ekane, D. N., & Oben, P. M. (2001). Biochemical indicators of marine pollution in the Douala lagoon and Limbe estuary. Environmental Issues. J. of the Univ. Buea.

El Morhit, M., Fekhaoui, M., Serghini, A., El Blidi, S., El Abidi, A., Yahyaoui, A. & Hachimi, M. (2012). Étude de l'évolution spatio-temporelle des paramètres hydrologiques caractérisant la qualité des eaux de l'estuaire du Loukkos (Maroc). Bul.Institut Scientifique, Rabat, section Sciences de la Vie. 34(2): 151-162.

ENVIREP-Cmr. (2011). Évaluation des impacts des activités pétrolières sur les écosystèmes de mangroves et les habitats côtiers, Colloque international en évaluation environnementale « Forêts, énergie, changement climatique et évaluation environnementale : pour une gestion durable, du global au local », 25 p.

Fernando, G. (2005). Histioneis (Dinophysiales, Dinophyceae) from the western Pacific Ocean. Botanica Marina 48(5-6): 421–425 by Walter de Gruyter Berlin New York. https://doi.org/10.1515/bot.2005.055

Folack, J., & Youmgbi, C. G. (2009). Surveillance des eaux cotières de la république du Cameroun. Rapport Final.

Folack, J. (2010). Résultats et Prospectives de recherches océanographiques en Afrique dédiées à l'Atlantique tropical et au Golfe de Guinée, Rapport CERECOMA-IRAD, 11p.

Folack, J. (2011). Mise en œuvre de la gestion intégrée des zones côtières (GIZC) pour la région de Kribi-campo au Cameroun. Rapport texte principal MINEP, pp43-47.

Fonge, A. B., Chuyong, B. G., Tening, A. S., Fobid, A. C., & Numbisi, N. U. (2013). Seasonal occurrence, distribution and diversity of phytoplankton in the Douala Estuary, Cameroon. *African Journal of Aquatic Science, 38*(2), 123–133. https://doi.org/10.2989/16085914.2013.769086

Fonge, B. A., Tening, A. S., Egbe, E. A., Yinda, G. S., Fongod, A. N., & Achu, R. M. (2012). Phytoplankton diversity and abundance in Ndop wetland plain, Cameroon, African Journal of African Journal of Aquatic Science, 6(6):247-257. https://doi.org/10.5897/AJEST12.025. ISSN 1996-0786.

Fretey, J., Triplet, P., Angoni, H., Ndouteng, N. X., Gnamaloba, D., Mediko, T., Mpinde, F., & Adjonina, G. (2022). Suivi de la nidifi cation des tortues marines dans le Parc national de Douala-Edea (Cameroun) comme étape préliminaire d'un plan de gestion. *African Sea Turtle Newsletter, 13*(2), 3–10.

Gharib, S. M., El-Sherif, Z. M., Abdel-Halim, A. M., & Radwan, A. A. (2011). Phytoplankton and environmental variables as a water quality indicator for the beaches at Matrouh, south-eastern Mediterranean Sea, Egypt: An assessment. *Oceanologia, 53*(3), 819–836. https://doi.org/10.5697/oc.53-3.819

Giresse, P. & Cahet, G. (1997). Organic fluxes of Cameroonian rivers into the Gilf of Guinea: a quantitative in estuary and plume, Oceanologica Acta 0399 1784/97/06. 20(6): 837-849.

Gopinathan, C. P., Gireesh, R., & Smitha, K. S. (2001). Distribution of chlorophyll *a* and *b* in the eastern Arabian Sea (west coast of India) in relation to nutrients during post monsoon. *Journal of the Marine Biological Association of India, 43*(1-2), 21–30.

Gordon, C. M. (1975). Sediment entrainment and suspension in a turbulent tidal flow. *Marine Geology, 18*(1), 57–64. https://doi.org/10.1016/0025-3227(75)90040-7

Gupta, G. V. M., Thottathil, S. D., Balachandran, K. K., Madhu, N. V., Madeswaran, P., & Nair, S. (2009). CO2 Supersaturation and net heterotrophy in a tropical estuary (Cochin, India) : Infiuence of Antropqgenic effect. *Ecosystems (New York, N.Y.), 12*(7), 1145–1157. https://doi.org/10.1007/s10021-009-9280-2

Houssou, A. M., Agadjihouédé, H., Bonou, C. A., & Montchowui, E. (2016), Composition and seasonal variation of phytoplankton community in Lake Hlan, Republic of Bénin, Int. J. Aquat. Biol. 4(6): 378-386: ISSN: 2322-5270; P-ISSN: 2383-0956.

Iltis, A. (1980). Les algues Hydro-biologiques (Vol. 1). ORSTOM.

Issifou, L., Atanlé, K., Radji, R., Lawson, H. L., Adjonou, K., Edorh, M. T., Kokutse, A. D., Mensah, A. A., & Kokou, K. (2014). Checklist of tropical algae of Togo in the Guinean Gulf of West-Africa. *Scientific Research and Essays, 9*(22), 932–958. https://doi.org/10.5897/SRE2014.6113

Jones, A. B., Dennison, W. C., & Preston, N. P. (2001). Integrated treatment of shrimp effluent by sedimentation, oyster filtration and macroalgal absorption: A laboratory scale study. *Aquaculture (Amsterdam, Netherlands), 193*(1-2), 155–178. https://doi.org/10.1016/S0044-8486(00)00486-5

Jouffre, D., Lam-Hoai, T., Millet, B., & Amanieu, M. (1991). Structure spatiale des peuplements zooplanctoniques et fonctionnement hydrodynamique en milieu lagunaire. *Oceanologica Acta, 14*(5), 489–504. 0399-1784/91/05 489

Chaudhuri, K., Manna, S., Sarma, K. S., Naskar, P., Bhattacharyya, S., & Bhattacharyya, M. (2012). Physicochemical and biological factors controlling water column metabolism in Sundarbans estuary, India. *Aquatic Biosystems, 8*(1), 26. https://doi.org/10.1186/2046-9063-8-26 PMID:23083531

Kadiri, M. O. (1999). Phytoplankton Distribution in some Coastal Water of Nigeria. *Nigerian Journal of Botany, 12*(1), 51–62.

Kaniz, F., Wan-Maznah, W. O., & Mansor, M. I. (2014). Limnology of Merbok Estuary, Kedah, Malaysia. *Bangladesh Journal of Zoology, 41*(1), 13–19.

Fatema, K., Wan Maznah, W. O., & Isa, M. M. (2014). Spatial and Temporal Variation of Physico-chemical Parameters in the Merbok Estuary, Kedah, Malaysia. *Tropical Life Sciences Research, 25*(2), 1–19. PMID:27073596

Karlson, B., Cusack, C., & Bresnan, E. (2010). Microscopic and molecular methods for quantitative phytoplankton analysis.- IOC Manuals and Guides, num. 55, IOC/2010/MG/5 UNESCO, Paris, France, 110 p.

Kebe, M., Njock, J. C., & Gallene, J. (1993). Revue xx sectorielle de la pêche artisanale maritime au Cameroun. Programme de Développement Intégré des Pêches Artisanales en Afrique de l'Ouest. DIPA.

Kokoette, S. E., & Aniefiok, I. I. (2016). Diversity of Phytoplankton in Iragbo Part of Yewa Lagoon, Southwest, Nigeria. American. *Journal of Bio-Science, 4*(4), 41–48. https://doi.org/10.11648/j.ajbio.20160404.11

Lam-Hoai, T., Amanieu, A., & Lassere, G. (1985). Communautés du zooplancton superficiel des trois sites différemment éloignés de l'entrée des eaux marines dans l'étang de Thau. *Cahiers de Biologie Marine, 26*(1), 445–467.

Lasserre, G., Sautter, G., Boyé, M., Brasseur, G., Réaud, G., Cabaussel, G., & Menault, J. (1979). Atlas des départements français d'Outre-Mer : 4. La Guyane. CNRS.

Legendre, L., & Demers, S. (1984). Towards dynamic biological oceanography and limnology. *Canadian Journal of Fisheries and Aquatic Sciences, 41*(1), 2–19. https://doi.org/10.1139/f84-001

Legendre, L., & Legendre, P. (1984). Ecologie numérique. Le traitement multiple des données écologiques. La structure des données écologiques. 2ème édition. Masson et Presses de l'Université du Québec.

Letouzey, R. (1985). Notice de la carte phytogéographique du Cameroun, 1: 500.000 4/TV: domaine de la forêt dense humide toujours verte - groupement 185 à 267, pp95-142.

Li, Y., Xu, L., & Li, S. (2009). Water Quality Analysis of the Songhua River Basin Using Multivariate Techniques. *Journal of Water Resource and Protection, 1*(2), 110–121. https://doi.org/10.4236/jwarp.2009.12015

Lienou, G. (2007). Impacts de la variabilité climatique sur les ressources en eau et les transports de matières en suspension de quelques bassins versants représentatifs au Cameroun. Thèse de doctorat, Univ. Yaoundé I, 486 p.

Maia de Oliveira, C. J., & Clavier, J. (2000). Variations spatio-temporelles des matieres en suspension dans l'estuaire du Sinnamary, Guyane Française. Influence du barrage hydroélectrique de Petit Saut. *Revista Brasileira de Oceanografia, 48*(1), 29–39. https://doi.org/10.1590/S1413-77392000000100003

Makombu, J. G., Oben, B. O., Oben, P. M., Makoge, N., Nguekam, E. W., Gaudin, G. L. P., Motto, I. S., Konan, K. M., Brown, J. H., Ngueguim, J. R., Mialhe, E., & Brummett, R. E. (2015). Biodiversity of species of genus: Macrobrachium (Decapoda, Palaemonidae) in Lokoundje, Kienké and Lobe Rivers of South Region, Cameroon. Journal of Biodiversity and Environmental Sciences (JBES) ISSN: 2220-6663 (Print) 2222-3045 (Online) 7(1): 68-80.

Makombu, J. G., Stomeo, F., Oben, P. M., Tilly, E., Stephen, O. O., Oben, B. O., Cheruiyot, E. K., Tarekegn, G. M., Zango, P., Egbe, A. E., Ndagyong, A., Mialhe, E., Ngueguim, J. R., & Mu-

jibi, F. D. N. (2019). Morphological and molecular characterization of freshwater prawn of genus *Macrobrachium* in the coastal area of Cameroon. *Ecology and Evolution, 9*(24), 14217–14233. https://doi.org/10.1002/ece3.5854 PMID:31938513

Mama, A. C., Bodo, W. K. A., Ghepdeu, G. F. Y., Ajonina, G. N., & Ndam, J. R. N. (2021). Understanding Seasonal and Spatial Variation of Water Quality Parameters in Mangrove Estuary of the Nyong River Using Multivariate Analysis (Cameroon Southern Atlantic Coast). *Open Journal of Marine Science., 11*(3), 103–128. https://doi.org/10.4236/ojms.2021.113008

Mama, A. C., Ghepdeu, G. F. Y., Ngoupayou Ndam, J. R., Bonga, M. D., Onana Fils, M., & Onguene, R. (2018). Assessment of water quality in the lower Nyong estuary (Cameroon, Atlantic Coast) from environmental variables and phytoplankton communities' composition. *African Journal of Environmental Science and Technology, 12*(6), 198–208. https://doi.org/10.5897/AJEST2017.2454

Mama, A. C., Oben, L. M., Dongmo, T. C., Ndam Ngoupayou, J. R., Motto, I., & Ayina, O. L. M. (2016). Tidal Variations and its Impacts on the Abundance and Diversity of Phyoplankton in the Nyong Estuary of Cameroon, JMEST, 3(1), ISSN: 3159-0040.

Mama, D. (2010). Méthodologie et Résultats Du Diagnostic de L'Eutrophisation Du Lac Nokoue (Bénin) (Thèse de Doctorat), Université de Limoge, Limoge, France.

Matiatos, I., Alexopoulos, A., & Godelitsas, A. (2014). Multivariate statistical analysis of the hydrogeochemical and isotopic composition of the groundwater resources in northeastern Peloponnesus (Greece). *The Science of the Total Environment, 476-477*, 577–590. https://doi.org/10.1016/j.scitotenv.2014.01.042 PMID:24496031

Maurizot, P., Abessolo, A., Feybesse, J. L., & Johan Lecomte, P. (1986). Etude de prospection minière du Sud-Ouest Cameroun. Synthèse des travaux de 1978 à 1985. Rapport de BRGM 1985, 274p.

Mayif, M. O. A. (1987). Un modèle estuarien limite : le Bou Regreg, (Maroc). Contribution à l'étude hydrodynamique, hydrologique, géochimique et minéralogique. Thèse de 3 ème cycle, E. N. S. Rabat (Maroc), 137 p.

McLusky, D. S., & Elliott, M. (2004). The Estuarine Ecosystem: Ecology, Threats and Management (3rd ed.). Oxford University Press. https://doi.org/10.1093/acprof:oso/9780198525080.001.0001

McLusky, D. S. (1981). The estuarine ecosystem. Blackie.

MINEF-CMR. (2005). Communication initiale sur les changements climatiques au Cameroun.

Monod, T. (1928). L'industrie de pêches au Cameroun. Société d'éditions. 504p.

Muduli, P. R., Vinithkumar, N. V., Begum, M., Robin, R. S., Vardhan, K. V., Venkatesan, R., & Kirubagarun, R. (2011). Spatial variation of hydrochemical characteristics in and around Port Blair Bay Andaman and Nicobar Islands, India. World Applied Sciences Journal 13(3) : 564-571. ISSN 1818-4952.

N'guessan, Y. A., Wango, T., Konan, K., Adingra, A., Etché, M. A. E., Monde, S., Affian, K., & Aka, K. (2015). Hydrologie et morphologie de l'estuaire du fleuve Sassandra, Basse Côte d'Ivoire. Afrique Science 11(2) : 161 – 172. ISSN 1813-548X.

Ndam Ngoupayou, J. R. (1997). Bilans hydrogéochimiques sous forêt tropicale humide en Afrique : du bassin expérimental de Nsimi-Zoétélé aux réseaux hydrogaphiques du Nyong et de la Sanaga (Sud-Cameroun). Thèse de doctorat, Univ. Pierre et Marie Curie, Paris VI, 214 p.

Ndjigui, P. D., Onana, V. L., Sababa, E., & Bayiga, E. C. (2018). Mineralogy and geochemistry of the Lokoundje alluvial clays from the Kribi deposits, Cameroonian Atlantic coast: Implications for their origin and depositional environment. *Journal of African Earth Sciences, 143*(1), 102–117. https://doi.org/10.1016/j.jafrearsci.2018.03.023

Njifonjou, O. (1998). Etude de la dynamique de l'exploitation dans la pêche artisanale maritime au Cameroun, Cah. D'OCISCA, 228p.

Nkoue, N.G.R. (2008). Le cycle du carbone en domaine tropical humide : exemple du bassin versant forestier du Nyong au Sud Cameroun, Université de Toulouse III Paul Sabatier, Université de Yaoundé 1.

Nlend Nlend. P.R. (2014). Les traditions ceramiques dans leur contexte archéologique sur le littoral camerounais (Kribi-Campo) de 3000 à 500 BP. Thèse de doctorat de l'Université Libre de Bruxelles.

Nwankwo, D. I. (1996). Phytoplankton diversity and succession in Lagos Lagoon, Nigeria. *Archiv für Hydrobiologie, 135*(4), 529–542. https://doi.org/10.1127/archiv-hydrobiol/135/1996/529

Oketola, A. A., Adekolurejo, S. M., & Osibanjo, O. (2013). Water Quality Assessment of River Ogun Using Multivariate Statistical Techniques. *Journal of Environmental Protection, 4*(5), 466–479. https://doi.org/10.4236/jep.2013.45055

Okosisi, F. A., & Akoma, O. C. (2012). Preliminary Checklist of Phytoplankton and Periphyton in River Okhuo, Nigeria. Current Research Journal of Biological Sciences 4(5): 538-543, 2012. ISSN: 2041-0778.

Olivry, J. C. (1986). Fleuves et rivières du Cameroun. Monographies hydrologiques. Mesres/Orstom.

Ong, F. S., & Ransangan, J. (2018). Assessment of Spatial and Temporal Variations of Water Quality for Future Mariculture Operation in Ambong Bay, Sabah, Malaysia. *Open Journal of Marine Science, 8*(1), 1–19. https://doi.org/10.4236/ojms.2017.81001

Opute, F. I. (2000). Contribution to the Knowledge of Algae of Nigeria I. Desmids from the Warri/Forcades Estuaries Part II. the Elongate Baculiform Desmids. *Journal of Limnology, 59*(2), 131–155. https://doi.org/10.4081/jlimnol.2000.131

Owona Edoa, F. D., Eneke Takem, G., Banga Medjo, P., Mama, A. C., Zambo, G. B., Kouedeum Kueppo, J. É., Safia Mahamat, T., & Zebaze Togouet, S. H. (2022). Spatio-Temporal Varia-

tion of Dinoflagellates of the Genera Ceratium (Schrank 1793) and Protoperidinium (Bergh 1881) in Relationship with Some Abiotic Variables in the Atlantic Coast of Kribi (South Region-Cameroon). *Open Journal of Marine Science, 12*(1), 161–184. https://doi.org/10.4236/ojms.2022.124010

Rachana, B.C. & Meenakshi, B.B. (2016). Mitigation of selenium toxicity by the immobilized cyanobacterium hapalosiphon sp from the rice field ecosystems. I.J.A.B.R. 6(4): 498-504. ISSN 2250 – 3579.

Rakotondrabe, F., Ndam Ngoupayou, J. R., Mfonka, Z., Rasolomanana, E. H., Nyangono Abolo, A. J., & Ako Ako, A. (2018). Water quality assessment in the Bétaré-Oya gold mining area (East-Cameroon): Multivariate Statistical Analysis approach. *The Science of the Total Environment, 610-611*(1), 831–844. https://doi.org/10.1016/j.scitotenv.2017.08.080 PMID:28826121

Reid, G. K. (1961). Ecology of inland waters and estuaries. New York : Van Nostrand Reinhold Company. ISBN 10: 0278919618. ISBN 13: 9780278919617

Riaux-Gobin, C. (1987). Phytoplankton, tripton et microphytobenthos: ´echanges au cours de la mareé, dans un estuaire du Nord-Finistere,Cahiers de Biologie Marine. 28(2): 159–184. ISSN 0007-9723

Rodier, J., Legube, B., & Merlet, N. (2009). L'analyse de l'eau. Paris, Dunod, 9e édition, 1579 p. ISBN : 978-2-10-075412-0.

Rossi, N. (2008). Ecologie des communautés planctoniques méditerranéennes et étude des métaux lourds (Cuivre, Plomb, Cadmium) dans déférents compartiments de deux écosystèmes côtiers (Toulon, France). These de doctorat de L'université du Sud Toulon-Var.

Ruperd, Y. (1983). Méthodes d'analyse biologiques des eaux douces superficielles. Bulletin de Liaison. Laboratoire de Physique et Chimie. 123 (1) : 109-116. ISBN 978-1-896997-79-7.

Samocha, T. M., & Lawrence, A. L. (1995). Shrimp farms effluent waters, environmental impact and potential treatment methods. In: Proceedings of 24th US–Japan Aquaculture Panel Symposium, october 8-10, 1995 (pp59-64). Corpus Christi, Texas.

Sanaa, B. (2006). Structure et dynamique du peuplement phytoplanctonique d'un estuaire atlantique marocain (estuaire de Bou Regreg): effets des conditions environnementales locales. Journal de Recherche Océanographique. 284p, http://toubkal.imist.ma/handle/123456789/191

Singh, K. P., Malik, A., Mohan, D., & Sinha, S. (2004). Multivariate statistical techniques for the evaluation of spatial and temporal variations in water quality of Gomti River (India)—A case study. *Water Research, 38*(18), 3980–3992. https://doi.org/10.1016/j.watres.2004.06.011 PMID:15380988

Soh Tamehe, L., Nzepang Tankwa, M., Wei, C. T., Ganno, S., Ngnotue, T., Kouankap Nono, G. D., Simon, S. J., Zhang, J. J., & Nzenti, J. P. (2018). Geology and geochemical constrains on the origin and depositional setting of Kpwa-Atog Boga banded iron formations (BIFs), northwestern Congo craton, southern Cameroon. *Ore Geology Reviews, 95*(1), 620–638. https://doi.org/10.1016/j.oregeorev.2018.03.017

Soininen, J. (2002). Response of epilithic diatom communities to environmental gradients in some Finnish rivers. *International Review of Hydrobiology, 87*(1), 11–24. https://doi.org/10.1002/1522-2632(200201)87:13.0.CO;2-E

Sokal, R. R., & Rohlf, F. J. (1995). Biometry: The Principles and Practice of Statistics in Biological Research (3rd ed.). W.H. Freeman and Co.

Sournia, A. (1978). Phytoplankton manual. Monographs on oceanographic methodology 6. Muséum National d'Histoire Naturelle. UNESCO.

Steidinger, K. A., & Tangen, K. (1996). Identifying marine diatoms and dinoflagellates. Academic Press, Inc., https://doi.org/10.5860/CHOICE.34-0289

Suman, M., Kaberi, C., Kakoli, S. S., Pankaj, N., Somenath, B., & Maitree, B. (2012). Interplay of Physical, Chemical and Biological Components in Estuarine Ecosystem with Special Reference to Sundarbans, India, Ecological Water Quality - Water Treatment and Reuse, Dr. Voudouris (Ed.), ISBN: 978-953-51-0508-4.

Tchakonté, S., Ajeagah, G. A., Diomande, D., Camara, I. A., & Ngassam, P. (2014b). Diversity, dynamic and ecology of freshwater snails related to environmental factors in urban and suburban streams in Douala-Cameroon (Central Africa). *Aquatic Ecology, 48*(4), 379–395. https://doi.org/10.1007/s10452-014-9491-2

Tchakonté, S., Ajeagah, G. A., Diomande, D., Camara, I. A., Konan, K. M., & Ngassam, P. (2014a). Impact of anthropogenic activities on water quality and Freshwater Shrimps diversity and distribution in five riversin Douala, Cameroon. J. Biodivers. Environ. Sci. 4(2): 183-194. ISSN: 2220-6663

Tilstone, G. H., Miguez, B. M., Figueiras, F. G., & Fermin, E. G. (2000). Diatom dynamics in ecosystem affected by upwelling: Coupling between species succession, circulation and biogeochemical processes. *Marine Ecology Progress Series, 205*(1), 23–41. https://doi.org/10.3354/meps205023

Tolomio, C., Andreoli, C., Darin, M., & Bortolotto, M. (1992). Le phytoplancton de surface dans la lagune d'Acquatina-Frigule (mer Adriatique méridionale). *Marine Life (Marseille), 2*(1), 47–52.

Yuri, B. O. (2014). Dinophysiales (Dinophyceae) of the National Park Sistema Arrecifal Veracruzano, Gulf of Mexico, with a key for indentification. Acta botánica Mexicana. ISSN 2448-7589.

Zeller, D., Cashion, T., Palomares, M. L. D., & Pauly, D. (2018). Global marine fisheries discards: A synthesis of reconstructed data. *Fish and Fisheries, 19*(1), 30–39. https://doi.org/10.1111/faf.12233